UNIVERSIDADE FEDERAL DE SANTA CATARINA
CENTRO TECNOLÓGICO
PROGRAMA DE PÓS-GRADUAÇÃO EM ENGENHARIA QUÍMICA

Luisa Isago Fusinato

Cobalt Doped Si-based Polymer-derived Ceramics for Sodium Borohydride Hydrolysis Reaction

Florianópolis
2023

Luisa Isago Fusinato

Cobalt Doped Si-based Polymer-derived Ceramics for Sodium Borohydride Hydrolysis Reaction

Dissertação submetida ao Programa de Pós-Graduação em Engenharia Química da Universidade Federal de Santa Catarina para a obtenção do título de mestre em Engenharia Química.
Orientador: Prof. Ricardo A. F. Machado, Dr.
Coorientadora: Emanoelle Diz Acosta, Drª.

Florianópolis
2023

Ficha de identificação da obra elaborada pelo autor,
através do Programa de Geração Automática da Biblioteca Universitária da UFSC.

Fusinato, Luisa Isago
Cobalt Doped Si-based Polymer-derived Ceramics for Sodium Borohydride Hydrolysis Reaction / Luisa Isago Fusinato ; orientador, Ricardo Antônio Francisco Machado, coorientadora, Emanoelle Diz Acosta, 2023.
71 p.

Dissertação (mestrado) - Universidade Federal de Santa Catarina, Centro Tecnológico, Programa de Pós-Graduação em Engenharia Química, Florianópolis, 2023.

Inclui referências.

1. Engenharia Química. 2. Polymer-derived ceramics. 3. Hydrogen. 4. Hydrolysis. I. Machado, Ricardo Antônio Francisco. II. Acosta, Emanoelle Diz. III. Universidade Federal de Santa Catarina. Programa de Pós-Graduação em Engenharia Química. IV. Título.

Luisa Isago Fusinato

Cobalt Doped Si-based Polymer-derived Ceramics for Sodium Borohydride Hydrolysis Reaction

O presente trabalho em nível de mestrado foi avaliado e aprovado por banca examinadora composta pelos seguintes membros:

Maíra Debarba Mallmann, Drª.
Universidade Federal de Santa Catarina (EQA)

Prof. Luiz Fernando Belchior Ribeiro, Dr.
Universidade Federal de Santa Catarina (FQM)

Certificamos que esta é a **versão original e final** do trabalho de conclusão que foi julgado adequado para obtenção do título de Mestre em Engenharia Química pela Universidade Federal de Santa Catarina.

ICP-Edu
Documento assinado digitalmente
Debora de Oliveira
Data: 08/12/2023 15:36:29-0300
CPF: ***.453.929-**
Verifique as assinaturas em https://v.ufsc.br

Profª. Débora de Oliveira, Drª.
Coordenadora do Programa

Prof. Ricardo A. F. Machado, Dr.
Orientador

ICP-Edu
Documento assinado digitalmente
Ricardo Antonio Francisco Machado
Data: 08/12/2023 14:49:20-0300
CPF: ***.377.139-**
Verifique as assinaturas em https://v.ufsc.br

Florianópolis, 18 de setembro de 2023.

ACKNOWLEDGEMENTS

A todos que de alguma maneira me auxiliaram no caminho até aqui, meu mais sincero agradecimento. Em especial à minha família que sempre me incentivou a estudar, pois o conhecimento liberta. Ao Renan, por tudo e pelos incontáveis momentos em que esteve comigo. Ao professor Ricardo pelo acolhimento e orientação. À Manu pela paciência, orientação e amizade. À Maíra pelos ensinamentos, contribuições e amizade. Aos colegas e aos amigos do laboratório pela compreensão e auxílios. Aos amigos que (de longe e de perto) me apoiaram e suportaram quando mais precisei, Karina, Renata, Vinícius e Lucas.

Esta pesquisa utilizou instalações do Laboratório Nacional de Nanotecnologia (LNNano), do Centro Nacional de Pesquisa em Energia e Materiais (CNPEM), uma Organização Social supervisionada pelo Ministério da Ciência, Tecnologia e Inovações (MCTI). A equipe da instalação é reconhecida pela assistência durante os experimentos.

À Universidade Federal de Santa Catarina (UFSC), por ser uma instituição de ensino pública, gratuita e de muita qualidade. Ao Programa de Pós-Graduação em Engenharia Química (PósENQ) e ao Departamento de de Engenharia Química e Engenharia de Alimentos (EQA) pelos recursos e estruturas fornecidas para a realização deste trabalho.

Ao Programa de Inovação em Hidrogênio Verde (iH2 Brasil), ao projeto H2Brasil e à GIZ Brasil pelo apoio financeiro.

À Coordenação de Aperfeiçoamento de Pessoal de Nível Superior (CAPES), e ao Conselho Nacional de Desenvolvimento Científico e Tecnológico (CNPq) pelo auxílio financeiro prestado.

"You never lose by keep on fighting, you always lose by giving up"
(Unknown author)

RESUMO

No contexto da transição energética e dos esforços para a descarbonização da economia, o hidrogênio (H_2) destaca-se como um vetor energético altamente versátil. Dentre os materiais de armazenamento de hidrogênio, os hidretos metálicos surgem como uma opção viável devido à sua alta capacidade de armazenamento de hidrogênio. Notavelmente, o borohidreto de sódio ($NaBH_4$) se destaca como um hidreto metálico proeminente. Tradicionalmente, metais nobres têm sido empregados como catalisadores para liberação de hidrogênio de $NaBH_4$ devido à sua alta eficiência. No entanto, estes metais são raros e caros, o que levou a uma maior atenção nos últimos anos para os metais de transição. Entre os catalisadores à base de metais de transição, os à base de cobalto são altamente atrativos devido à sua alta atividade e baixo custo. A hidrólise do $NaBH_4$ é considerada severa em termos de condições químicas, levando à deterioração estrutural de muitos suportes catalíticos. Assim, o desenvolvimento de suportes catalíticos que possam suportar tais condições sem perder a atividade catalítica, preferencialmente com possibilidade de recuperação para reutilização, tem sido um desafio recente. Cerâmicas avançadas, particularmente aquelas produzidas através da rota Polymer-Derived Ceramic (PDC), são candidatas proeminentes no campo de suportes catalíticos. Utilizando esta rota é possível obter materiais onde a estrutura do silício pode ser dopada com nanocristais metálicos para atuarem como catalisadores, apresentando uma abordagem promissora na área de suportes catalíticos. Neste estudo, foram desenvolvidos três materiais cerâmicos derivados de polímeros dopados com cobalto. Utilizou-se cloreto de cobalto (II) como precursor metálico e três polímeros pré-cerâmicos: alilhidridopolicarbosilano (AHPCS), peridropolissilazano (PHPS) e poli(metilvinil)silazano (HTT). A caracterização dos materiais foi feita por análises de TGA, FTIR, XRD e XPS. Os resultados mostraram que cerâmicas à base de silício dopadas com cobalto foram obtidas com sucesso pela rota PDC. Os materiais produzidos foram testados na reação de hidrólise de borohidreto de sódio para avaliar sua atividade catalítica, resultando em taxas variadas de geração de hidrogênio nas quatro temperaturas testadas. Os valores variaram de 34 a 7.641 mL min^{-1} $g^{-1}{}_{cat}$, com o melhor resultado sendo de 7.641 mL min^{-1} $g^{-1}{}_{cat}$ para o catalisador PHCo2.5 testado a 353 K. Além disso, este catalisador passou por testes contínuos de reutilização, com resultados interessantes. Após quatro ciclos de uso contínuo, foi observada apenas uma diminuição de 26% na conversão de $NaBH_4$. O catalisador foi então lavado com água deionizada e submetido novamente à reação de hidrólise, resultando em uma diminuição de 29% na conversão após quatro ciclos. Estes resultados demonstram que os materiais produzidos têm potencial para serem explorados como suportes catalíticos para a reação de hidrólise do borohidreto de sódio. Espera-se que este trabalho contribua para o desenvolvimento de novas tecnologias no contexto de um futuro baseado em fontes de energia limpas e em vetores energéticos renováveis como o hidrogênio.

Palavras-chave: Cerâmicas derivadas de polímeros; Hidrogênio; Hidrólise.

ABSTRACT

In the context of energy transition and efforts towards decarbonizing the economy, hydrogen (H_2) stands out as a highly versatile energy carrier. Among hydrogen storage materials, metal hydrides emerge as a viable option due to their high hydrogen storage capacity. Notably, sodium borohydride ($NaBH_4$) stands out as a prominent metal hydride. Traditionally, noble metals have been employed as catalysts for releasing hydrogen from $NaBH_4$ due to their high efficiency. However, these metals are rare and expensive, prompting increased attention in recent years towards transition metals. Among transition metal-based catalysts, cobalt-based ones are highly attractive due to their high activity and low cost. The hydrolysis of $NaBH_4$ is considered harsh in terms of chemical conditions, leading to the structural deterioration of many catalytic supports. Hence, developing catalytic supports that can withstand such conditions without losing catalytic activity, preferably with the possibility of recovery for reuse, has been a recent challenge. Advanced ceramics, particularly those produced through the Polymer-Derived Ceramic (PDC) route, are prominent candidates in the field of catalytic supports. Utilizing this route, it is possible to obtain materials where the silicon structure can be doped with metal nanocrystals to act as catalysts, presenting a promising approach in the field of catalytic supports. In this study, three cobalt-doped polymer-derived ceramic materials were developed. cobalt (II) chloride was employed as metallic precursor and three preceramic polymers: Allylhydridopolycarbosilane (AHPCS), Perhydropolysilazane (PHPS), and Poly(methylvinyl)silazane (HTT). Characterization of the materials was done by TGA, FTIR, XRD and XPS analysis. Results showed that cobalt-doped silicon-based ceramics were successfully obtained via the PDC route. The produced materials were tested in the sodium borohydride hydrolysis reaction to assess their catalytic activity, resulting in different hydrogen generation rates at the four tested temperatures. The values ranged from 34 to 7641 mL min^{-1} $g^{-1}{}_{cat}$, with the best result of 7641 mL min^{-1} $g^{-1}{}_{cat}$ for the PHCo2.5 catalyst tested at 353 K. Moreover, this catalyst underwent continuous reuse testing, with interesting results. After four cycles of continuous use, only a 26% decrease in $NaBH_4$ conversion was observed. The catalyst was then washed with deionized water and subjected to the hydrolysis reaction again, resulting in a 29% decrease in conversion after four cycles. These results demonstrate that the materials produced have the potential to be explored as catalytic supports for the sodium borohydride hydrolysis reaction. It is expected that this work will contribute to the development of new technologies in the context of a future based on clean energy sources and renewable energy vectors such as hydrogen.

Keywords: Polymer-derived ceramics; Hydrogen; Hydrolysis.

RESUMO EXPANDIDO

Introdução

No contexto da transição energética e do esforço para a descarbonização da economia, o hidrogênio (H_2) se destaca como um vetor energético altamente versátil. Para um futuro sustentável, a abordagem mais promissora envolve o aproveitamento de fontes de energia renováveis, juntamente com tecnologias de ponta em desenvolvimento para a produção de hidrogênio. Dentre os materiais armazenadores de H_2, os hidretos metálicos surgem como uma opção viável devido à sua alta capacidade de armazenamento de hidrogênio. Notavelmente, o borohidreto de sódio ($NaBH_4$) se destaca como um hidreto metálico proeminente, capaz de fornecer até 4 mols de hidrogênio por mol de hidreto. Tradicionalmente, metais nobres têm sido empregados como catalisadores na liberação de hidrogênio a partir de $NaBH_4$ devido à sua alta eficiência. Porém, esses metais são raros e caros e por isso, os metais de transição têm ganhado atenção nos últimos anos por suas propriedades catalíticas na hidrólise de $NaBH_4$. Dentre os catalisadores à base de metais de transição, aqueles à base de cobalto são muito atrativos devido à sua alta atividade e ao também ao baixo custo. A reação de hidrólise do $NaBH_4$ é considerada severa em termos de condições químicas e por isso muitos suportes catalíticos tendem a sofrer deterioração estrutural. Portanto, nos últimos anos tem sido um desafio desenvolver suportes catalíticos que possam resistir a tais condições sem perder atividade catalítica e preferencialmente com possibilidade de recuperação, para reaproveitamento. No campo dos suportes catalíticos, as cerâmicas avançadas surgiram como candidatas proeminentes, particularmente aquelas produzidas através da rota PDC, do inglês *Polymer-Derived Ceramic*. Utilizando esta rota, é possível obter materiais onde a estrutura do silício pode ser dopada com metais na forma de nanocristais, para atuarem como catalisadores, trazendo uma abordagem promissora no cenário dos suportes catalíticos.

Objetivos

O presente trabalho tem como objetivo principal o desenvolvimento de cerâmicas derivadas de polímeros dopadas com cobalto para utilização na reação de hidrólise do borohidreto de sódio. Os objetivos específico são (i) a produção das PDC dopadas com cobalto a partir de três diferentes polímeros pré-cerâmicos (AHPCS, HTT e PHPS), utilizando cloreto de cobalto (II) como precursor metálico; (ii) avaliar as propriedades químicas, térmicas e estruturais dos materiais produzidos e (iii) testar a atividade catalítica dos materiais na reação de hidrólise do borohidreto de sódio.

Metodologia

A síntese das cerâmicas derivadas de polímeros e sua dopagem com cobalto foi realizada em solução com tolueno, polímero pré-cerâmico e o cloreto de cobalto (II), adotando a rota PDC como metodologia de síntese. Três diferentes polímeros pré-cerâmicos foram utilizados: alilhidridopolicarbosilano (AHPCS), Perhidropolisilazano (PHPS) e Poli(metilvinil)silazano (HTT). O manuseio dos reagentes e a síntese foi realizada sob atmosfera inerte de argônio utilizando técnicas Schlenk padrão devido à sensibilidade dos reagentes ao contato com oxigênio. Após a síntese, foi realizada a extração do solvente sob diferença de pressão e de temperatura, e o polímero em pó

resultante foi submetido a tratamento térmico sob atmosfera de argônio, com taxa de aquecimento de 5 °C min^{-1}, até 1000 °C com tempo de residência de uma hora nesta temperatura. Após ceramização, a atividade catalítica dos materiais produzidos foi averiguada através de seu uso na reação de hidrólise do $NaBH_4$. Utilizou-se o método de deslocamento de água para a medição dos volumes gerados de H_2. O teste foi feito adicionando-se uma quantidade conhecida de catalisador ao sistema, seguido da adição de $NaBH_4$, de NaOH e de água. O sistema era então imediatamente fechado e o gás H_2 gerado, deslocava a água para o recipiente que estava sendo pesado. Com isso, o volume de água deslocado é igual ao volume de H_2 gerado. O teste de reuso dos catalisadores foi realizado de maneira contínua, adicionando-se novas cargas de quantidade conhecida de $NaBH_4$, NaOH e água no sistema, mantendo-se a temperatura e o mesmo catalisador já utilizado anteriomente. Após, o catalisador foi lavado com água deionizada e centrifugado por cinco vezes com o intuito de lavar os boratos formados como co-produtos na reação. Após cinco lavagens, o catalisador foi seco e submetido novamente ao teste na reação de hidrólise.

Resultados e Discussão

As cerâmicas produzidas foram submetidas a análise termogravimétrica (TGA) onde foi possível observar perdas de massa condizentes com aquelas relatadas na literatura, que indicam a ocorrência das reações de cross-linking, e também um maior rendimento cerâmico quando comparado aos polímeros precursores puros. A análise de espectroscopia na região do infravermelho (FTIR) foi realizada com o polímero recém sintetizado e com tratamento térmico em diferentes temperaturas (200, 400 e 600 °C). Com os resultados obtidos, observou-se diminuição nas bandas referentes às ligações CH_3-CH_3, SiH_4 e CH_3-SiH_3 no **AHCo2.5**, referentes às ligações N-H e Si-H no **HTCo2.5** e por fim às ligações N-H, Si-N e Si-H de **PHCo2.5**. Estes resultados concordam com os obtidos por TGA E Confirmam a ocorrência de reações de cross-linking com liberação dos compostos correspondentes, e indicam o início da ceramização dos materiais. As cerâmicas foram analisadas por difração de raios-X (XRD) para a identificação das fases cristalinas presentes. Foram observados picos referentes ao cobalto na fase cúbica para os três materiais, indicando a presença do metal na mmatriz cerâmica produzida. Além disso, picos referentes ao monosiliceto de cobalto (CoSi) foram observados no **AHCo2.5** e picos de CoSi e siliceto de dicobalto (Co_2Si) para o material **PHCo2.5**. Análises de espectroscopia de fotoelétrons excitados por raios-X (XPS) foram realizadas nas cerâmicas produzidas. A atividade catalítica das cerâmicas foi testada na reação de hidrólise do borohidreto de sódio. Foram obtidos valores de taxa de geração de hidrogênio (HGR, do inglês *Hydrogen Generation Rate*) entre 34 e 7641 mL min^{-1} $g_{cat}{}^{-1}$ dentre as quatro diferentes temperaturas testadas (25, 40, 60 e 80 °C), e também valores próximos a 100% de conversão de $NaBH_4$ em H_2 na temperatura de 80 °C. O material **PHCo2.5** obteve o maior valor de HGR de 7641 mL min^{-1} $g_{cat}{}^{-1}$a 80 °C, e por isso foi utilizado para os testes de reuso. Após o primeiro uso, foi feita a adição de novas cargas de $NaBH_4$, NaOH e água no sistema e após 4 ciclos de uso consecutivos, houve uma queda de 26% na conversão de $NaBH_4$ em H_2. Este comportamento também foi relatado na literatura e deve estar relacionado à deposição dos boratos formados na reação sobre o catalisador, levando a uma diminuição no acesso aos sítios ativos. Portanto, foi utilizado procedimento de sucessivos ciclos de lavagem do catalisador com água deionizada, seguido de centrifugação na tentativa de reativar o catalisador. Após lavagem, o **PHCo2.5** foi submetido novamente à rea-

ção de hidrólise do $NaBH_4$. Desta vez, observou-se uma perda de 29% na conversão, sugerindo que a lavagem com água não é suficiente para a reativação do catalisador.

Considerações Finais

Neste trabalho foram desenvolvidos três materiais cerâmicos derivados de polímeros dopados com cobalto. Eles foram dopados com cobalto a partir de cloreto de cobalto (II) e produzidos a partir de três polímeros pré-cerâmicos: Alilhidridopolicarbosilano (AHPCS), Peridropolissilazano (PHPS) e Poli(metilvinil)silazano (HTT). As caracterizações realizadas no material mostraram que cerâmicas à base de silício dopadas com cobalto foram obtidas com sucesso pela rota PDC. Os materiais produzidos foram testados na reação de hidrólise do $NaBH_4$, a fim de testar sua atividade catalítica, onde apresentaram diferentes gerações de hidrogênio nas quatro temperaturas testadas. Os valores da taxa de geração de hidrogênio foram obtidos na faixa de 34 a 7641 mL min^{-1} $g_{cat}{}^{-1}$, sendo o melhor resultado 7641 mL min^{-1} $g_{cat}{}^{-1}$ para o catalisador **PHCo2.5** testado a 80 ℃ (353 K). Além disso, este catalisador foi submetido a testes contínuos de reutilização. Resultados interessantes foram obtidos, onde após quatro ciclos de uso contínuo, o catalisador apresentou queda de 26% na conversão de $NaBH_4$ em H_2. O catalisador foi então lavado com água sucessivas vezes para remoção de boratos (coprodutos da reação de hidrólise) e após secagem foi testado novamente na reação. Desta vez, após quatro ciclos de uso, o material apresentou queda de 29% na conversão, o que mostra que apenas a lavagem com água não foi suficiente para reativar o catalisador. Os resultados obtidos mostram que os materiais produzidos possuem bom potencial para serem explorados para serem utilizados como suportes catalíticos para a reação de hidrólise do $NaBH_4$. Os suportes catalíticos produzidos através da rota PDC são materiais muito promissores e espera-se que este trabalho contribua para o desenvolvimento de novas tecnologias no contexto de um futuro baseado em fontes de energia limpas e vetores de energia renováveis como o hidrogênio.

Palavras-chave: Cerâmicas derivadas de polímeros; Hidrogênio; Hidrólise.

LIST OF FIGURES

LIST OF TABLES

LIST OF ABBREVIATIONS AND ACRONYMS

AHPCS	Allylhydridopolycarbosilane
CNPEM	*Centro Nacional de Pesquisa em Energia e Materiais*
EQA	Departament of Chemical Engineering
FTIR	Fourier-Transformed Infrared Spectroscopy
HGR	Hydrogen Generation Rate
HS	Hydrogen Storage
HTT	Poly(methylvinyl)silazane
PDC	Polymer Derived Ceramics
PHPS	Perhydropolysilazane
SMR	Steam Methane Reforming
TGA	Thermogravimetric Analysis
TM	Transition Metals
UFSC	*Universidade Federal de Santa Catarina*
WE	Water Electrolysis
XPS	X-ray Photoelectron Spectroscopy
XRD	X-ray Diffraction Analysis

CONTENTS

1 INTRODUCTION

In the context of the ongoing energy transition and the drive towards decarbonizing economy, hydrogen (H_2) stands out as a highly versatile energy carrier and a promising alternative fuel for powering various sectors, including transportation. Its remarkable attribute of possessing the highest energy density among all known fuels has attracted significant international attention in recent years. To pave the way for a sustainable future, the most promising approach involves harnessing established renewable energy sources alongside cutting-edge technologies currently being developed for hydrogen production.

The distribution and storage of hydrogen pose significant challenges for its widespread utilization. H_2 storage can be accomplished using various methods, which can be broadly classified into two main categories: physical-based and material-based (solid-state) approaches. Among these, solid-state storage holds particular promise as it enables the storage of large quantities of hydrogen in a compact space. Within the solid-state storage materials, metal hydrides have emerged as a viable option due to their high hydrogen storage capacity. Notably, sodium borohydride ($NaBH_4$) stands out as a prominent metal hydride, capable of providing up to 4 moles of hydrogen per mole of hydride. Furthermore, it is relatively accessible and easy to handle, further enhancing its appeal as a potential storage solution.

The release of hydrogen from sodium borohydride ($NaBH_4$) requires the use of catalysts to enhance the hydrogen generation rate. Traditionally, noble metals like platinum, gold, and ruthenium have been employed as catalysts due to their effectiveness. However, these metals are rare and consequently expensive. As a result, transition metals (either alone or in combination with noble metals), have gained attention in recent years for their catalytic properties in $NaBH_4$ hydrolysis as they stand out for being more accessible, inexpensive and still efficient when comparing to noble metals. Among the catalysts based on transition metals, those based on cobalt are very attractive due to their high activity for hydrolysis reaction as well as low cost.

The $NaBH_4$ hydrolysis reaction is considered severe in terms of chemical conditions. This is because its co-products are strong bases, making the pH of the reaction medium excessively alkaline. Under these conditions, many catalytic supports end up suffering structural deterioration. Therefore, in recent years it has been a challenge to develop catalytic supports which can resist the severe conditions of the hydrolysis reaction without losing catalytic activity and preferably with the possibility of recovery, for reuse.

In the field of catalytic supports, advanced ceramics have emerged as prominent candidates, particularly those produced via the Polymer-Derived Ceramic (PDC) route, mainly due to their chemical stability. This route also allows molecular control of the final ceramic, enabling chemical and structural modifications. By utilizing PDC route, it is possible to obtain materials such as silicon carbide, silicon nitride or silicon carbonitride, for example, depending on the molecular structure of chosen preceramic polymer. During synthesis steps, the silicon backbone can be doped with metals in the form of nanocrystals, and thus the final ceramics can be used as catalysts.

Taking into account the preceding, this master's research proposes the creation of cost-effective cobalt-doped Polymer-Derived Ceramics as candidates for catalysts to use in $NaBH_4$ hydrolysis reaction, by modifying the types of preceramic polymers, based on the hypothesis:

If Polymer-Derived Ceramics exhibit robust characteristics as catalyst supports

and cobalt presents high catalytic activity, the synthesis of cobalt-doped Polymer-Derived Ceramics could yield catalysts with significant potential for releasing H_2 from the $NaBH_4$ through hydrolysis reaction.

1.1 OBJECTIVES

1.1.1 General Objective

Develop and characterize cobalt-doped polymer-derived ceramics, varying the type of preceramic polymer, and test their performance as catalysts supports in the sodium borohydride hydrolysis reaction.

1.1.2 Specific Objectives

• To synthesize cobalt-doped polymer-derived ceramics, using three different preceramic polymers namely Allylhydridopolycarbosilane (AHPCS), Perhydropolysilazane (PHPS), and Poly(methylvinyl)silazane (HTT).

• To evaluate the chemical, thermal and structural properties of the produced materials.

• To test the catalytic activity of produced materials using the sodium borohydride hydrolysis reaction.

• To test the reusability of the produced materials as catalysts.

2 LITERATURE REVIEW

2.1 CLEAN ENERGY

According to the 6th report of the Intergovernmental Panel on Climate Change - IPCC (2023), the impacts of human-caused climate change are already being felt across various regions, resulting in extensive damage to both the environment and human populations. It is necessary an immediate focus on the development of technologies pertaining to fuels and energy sources that generate minimal, or ideally, zero carbon emissions (IEA, 2023; IPCC, 2023).

The utilization of alternative fuels and renewable energy sources has become an imperative rather than a choice. To replace the reliance on fossil fuels across transportation, households and industries, the most viable approach appear to be the use of electric power and hydrogen. The synergistic integration of these two technologies has led to significant progress in terms of both efficiency and cost-effectiveness. This is evidenced by the substantial increase in investments and research activities within this sector across various countries, including Canada, the United States, China, Australia, and others. Moreover, there has been a notable surge in research dedicated to exploring and advancing these interrelated fields (PANCHENKO et al., 2023; ISHAQ et al., 2022; ARSAD et al., 2022; MAROCCO et al., 2022).

2.1.1 Hydrogen

In the context of the energy transition and the economy decarbonization, hydrogen (H_2) is a versatile energy carrier and a promising fuel to power and transportation. It is gaining international attention in the past years, due to its main feature of having the highest energy density compared to any other fuel. The most promising path seems to be the combination between the already known renewable energy sources and the technologies under development for hydrogen generation. By 2050, H_2 is expected to account 10% of global energy consumption, and in transport, it is expected to account 60% of ship fuel and for 33% of truck fuel (DOE, 2023; IEA, 2023; NNABUIFE et al., 2022).

Unlike oil, natural gas, or coal, H_2 serves as an environmentally friendly and beneficial energy carrier, as its only byproduct during energy conversion is water. Moreover, hydrogen exhibits natural compatibility with fuel cells, showing superior efficiency (60%) compared to gasoline (22%) or diesel (45%) (DAWOOD et al., 2020; ACAR; DINCER, 2020).

At present, approximately 80% of the global demand in hydrogen production is carried out by Steam Methane Reforming (SMR), and it is widely recognized as the most common and cost-effective method for hydrogen production. The majority of the produced H_2 is utilized in ammonia and petrochemical industries. In order to enhance the comprehension of the environmental impact of hydrogen as a clean energy source, it is classified into different colors based on its origin, production process and carbon dioxide (CO_2) emissions. The literature reports several classification schemes, one of which can be observed in Figure 1, presenting eight different colors (STANWELL, 2023; ARCOS; SANTOS, 2023; BARTLETT; KRUPNICK, 2020; DAWOOD et al., 2020).

Figure 1 – Hydrogen colors classification.

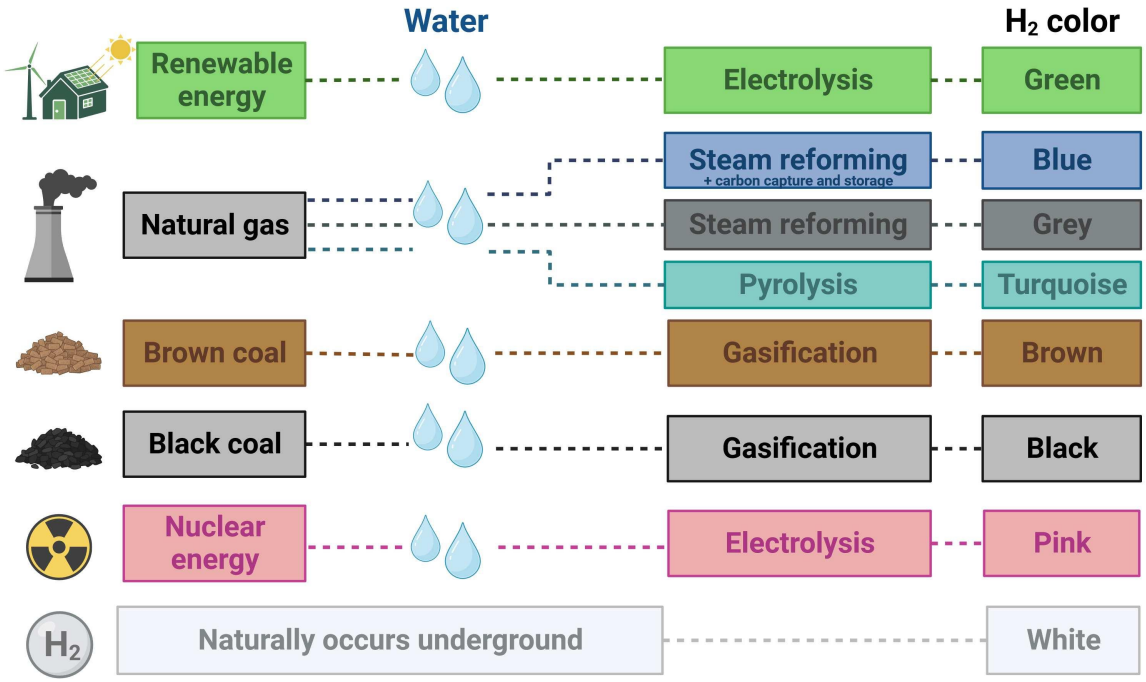

Source: Adapted from (STANWELL, 2023)

Another example of hydrogen classification can be found in Table 1, where four colors are presented, differing slightly from the previous example. Additional classifications mention hydrogen colors such as purple or pink (produced with nuclear energy), white (naturally occurring hydrogen), or even black instead of gray hydrogen (from the gasification process). Numerous other works also propose different classifications. However, when it comes to classifying "green hydrogen," there is consensus regarding the production process and its environmentally friendly nature. Green hydrogen is primarily produced from water, utilizing renewable energy sources like solar and wind power, by Water Electrolysis (WE). This process ensures a carbon footprint equal to zero (INCER-VALVERDE et al., 2023; HERMESMANN; MÜLLER, 2022; OSMAN et al., 2022; AJANOVIC et al., 2022).

Table 1 – Hydrogen colors based on production process.

Color	Gray	Turquoise	Blue	Green
Primary feedstock	Natural gas	Natural gas	Natural gas	Water
Production Technology	SMR	SMR + CCS	Methane pyrolysis	WE
CO_2 emissions	High CO_2	Low CO_2	CO_2 free	Carbon-free

Source: Adapted from Hermesmann and Müller (2022).

Another widely recognized consensus is that the current reliance on natural gas, methane, and coal for hydrogen production leads to significant CO_2 emissions. Presently, the majority of hydrogen production falls under the category of gray H_2, since 95% of production uses non-renewable fossil fuels, resulting in a total CO_2 formation of approximately 830 $MtCO_2$ per year, according to Kumar and Lim (2022). This information highlights the significance of green hydrogen (also referred to as "clean hydrogen", "renewable hydrogen", or "low-carbon hydrogen") in the transition towards

a more sustainable energy and transport system (IEA, 2023; INCER-VALVERDE et al., 2023; KUMAR; LIM, 2022).

Beyond promoting environmentally friendly hydrogen production, research on the hydrogen production chain should also consider other crucial aspects, with particular attention to storage. Hydrogen Storage (HS) plays a crucial role in the advancement of hydrogen and fuel cell technologies across various applications and is one of the obstacles to overcome. While H_2 presents the highest energy per mass among all fuels, its low density at room temperature limits its energy density per unit volume. Consequently, achieving optimized storage and efficient transport of hydrogen becomes imperative for its widespread utilization. Furthermore, ensuring safety in both transportation and storage is paramount to garner public acceptance of this innovative technology (KOJIMA, 2019; MORADI; GROTH, 2019).

H_2 storage can be accomplished using various methods, which can be broadly classified into two main categories: physical-based and material-based approaches. Figure 2 provides a schematic representation of this classification. Recent research has shown significant interest in solid-state materials, including complex hydrides, liquid organics, adsorbents, and nanostructured materials, which fall into the material-based category. Among these options, complex hydrides exhibit great potential due to their high hydrogen storage capacity. Notably, sodium borohydride ($NaBH_4$) stands out as a particularly remarkable hydride (DOE, 2023; MORADI; GROTH, 2019).

Figure 2 – Hydrogen storage main classification.

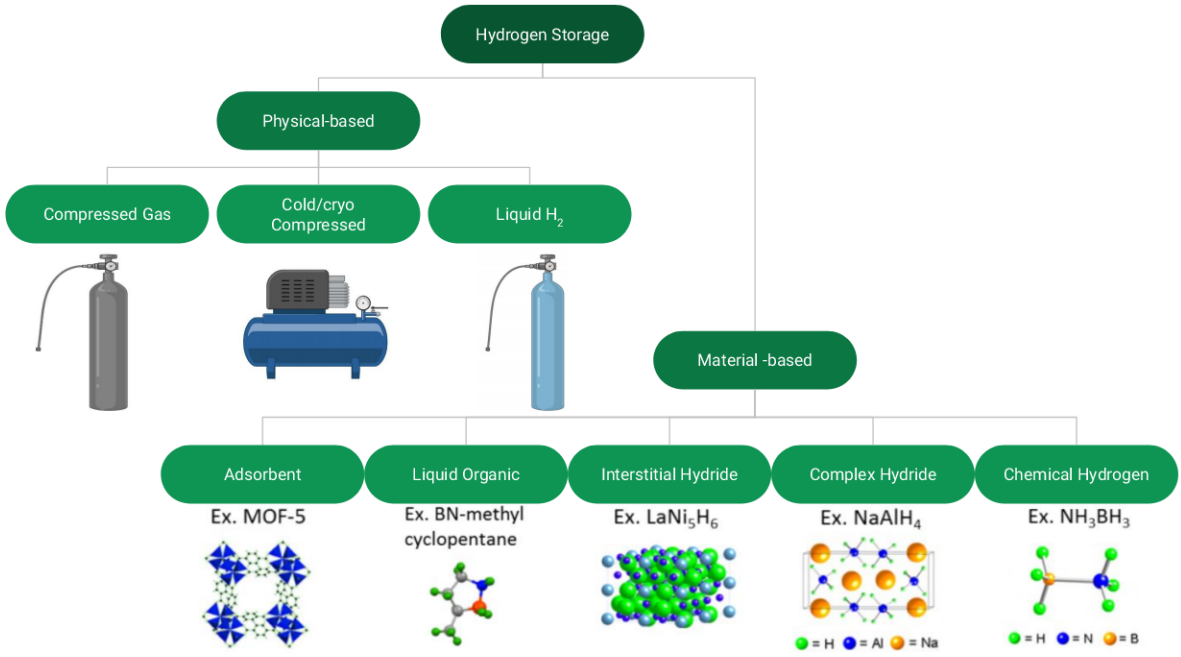

Source: Adapted from DOE (2023).

2.1.2 Sodium borohydride and its Hydrolysis Reaction

Many solid-state hydrogen storage materials release hydrogen by using hydrolysis reactions. Sodium borohydride ($NaBH_4$) offers numerous benefits such as cost-effectiveness, ease of handling, non-toxicity, non-flammability and environmental friend-

liness. In addition, sodium borohydride also offers the benefit of high volumetric and gravimetric hydrogen densities with values of 7 kg/100 L and 10.8% wt, respectively, as shown in Figure 3. These values surpass those of other metal hydrides (SONG et al., 2023; TARHAN; ÇIL, 2021; MAKIABADI et al., 2020; KOJIMA, 2019).

Despite its advantages, the solution-based storage system using $NaBH_4$ faces inherent limitations in terms of gravimetric capacity, typically restricted to less than 10.8% (wt%) due to the requirement for excess water to dissolve the produced sodium borates. Additionally, it exhibits slow kinetics, resulting in a low hydrogen yield. The self-hydrolysis reaction of $NaBH_4$ is both exothermic (-250 kJ mol^{-1}) and spontaneous. Nevertheless, under normal pressure and temperature conditions, the overall conversion rate is only 7-8%. However, with the inclusion of a suitable catalyst at moderate temperatures, 1 mole of $NaBH_4$ has the potential to yield up to 4 moles of H_2. Consequently, short-term applications of sodium borohydride for hydrogen storage are likely to concentrate on compact, portable devices and backup power systems, utilizing a fitting catalyst and dry $NaBH_4$, with water introduced only when necessary (LI, Y. et al., 2023; ECER et al., 2023; ABDELHAMID, 2021; LALE et al., 2020).

Figure 3 – Theoretical gravimetric and volumetric H_2 densities of hydrides.

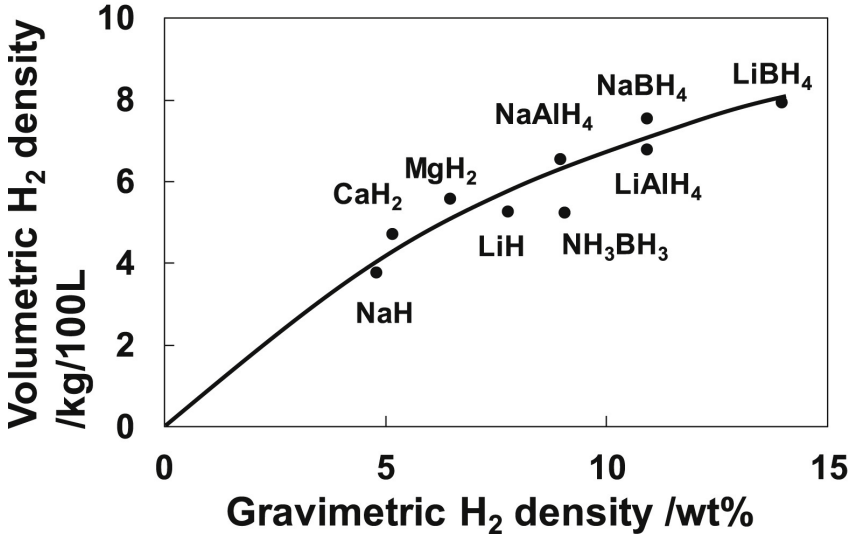

Source: Kojima (2019).

The pioneering work of Schlesinger et al. (1953) marked the initial demonstration of hydrogen evolution through the hydrolysis of sodium borohydride. Since then, numerous studies have been conducted to enhance the reaction's efficiency by employing catalysts. Ideally, the stoichiometry of the reaction yields the generation of 4 moles of H_2 for every mole of $NaBH_4$ utilized, as illustrated in Equation 1.

$$NaBH_{4(s)} + 4\,H_2O_{(l)} \rightarrow 4\,H_{2(g)} + Na^{+}_{(aq)} + B(OH)^{-}_{4(aq)} + \text{heat} \quad (1)$$

The hydrolysis of $NaBH_4$ is a spontaneous reaction, although with a low H_2 generation rate that decreases as the reaction progresses, primarily due to an increase in the pH of the solution caused by the formation of borates. To prevent spontaneous reaction, the solution can be stabilized by adding NaOH. However, once the $NaBH_4$ solution is stabilized, catalysis is necessary to promote hydrogen generation. Considering

an aqueous alkaline system and the requirement for a durable catalyst to facilitate the hydrolysis of $NaBH_4$ at appreciable rates, extensive research has been conducted to develop such catalysts. Among them, those based on cobalt have garnered significant attention due to their high abundance and relatively low cost. However, their catalytic activity is lower compared to catalysts containing noble metals, posing a significant challenge to be overcome in this research field (ECER et al., 2023; ARZAC, G. M.; FERNÁNDEZ, 2020; MAKIABADI et al., 2020; CHEN, B. et al., 2018; DEMIRCI, U. B.; MIELE, P., 2010).

Many published works employ oxide or carbon-based materials as supports. While these materials offer commendable properties, they encounter limitations under harsh conditions, like high temperatures and strongly alkaline environments. In order to surpass this challenge, it becomes imperative to explore catalytic supports for $NaBH_4$ hydrolysis capable of enduring such rigorous reaction conditions while maintaining high Hydrogen Generation Rate (HGR). This investigation is crucial for accelerating the advancement of hydrogen technology (MALLMANN, M. D., 2020).

Among the promising material that can be employed as catalyst supports, advanced ceramics, specially PDC, stand out as materials with a versatile composition and attractive physico-chemical characteristics for this purpose. Thus, the following section offers an overview of PDC for context.

2.2 POLYMER DERIVED CERAMICS (PDC)

PDC are a class of advanced ceramics characterized by a silicon-based backbone, exhibiting a remarkable combination of properties and the ability to be molded into diverse shapes, which production follows a specific methodology known as the PDC route, primarily reported by Ainger and Herbert (1959). The fundamental principle of the PDC route is around the creation of ceramics, typically non-oxide ceramics, via the thermo-chemical conversion of inorganic or organometallic precursors, referred to as preceramic polymers (CHAUDHARY et al., 2022; WEN et al., 2020; LALE et al., 2018).

In the field of materials science, the potential of preceramic polymers remained largely unrecognized until the 1970s when the first practical application was reported by Verbeek and Winter (1974), Gerhard Winter et al. (1975) and YAJIMA et al. (1978). They successfully manufactured small-diameter Si_3N_4/SiC-based and SiC-based ceramic fibers through the thermolysis of polyorganosilicon precursors. Since then, the development of numerous preceramic polymers and the increasing attention given to PDC have become prominent in recent decades, particularly in recent years, with a growing number of publications on the subject (WEN et al., 2020).

A generic representation of the molecular structure of preceramic organosilicon compounds can be observed in Figure 4. The choice of group (X) in Si-based polymers leads to the formation of distinct classes, including poly(silazanes) (when X = NH), poly(silanes) (when X = Si), poly(carbosilanes) (when X = CH_2), poly(siloxanes) (when X = O), and so on. Through the manipulation of functional groups R_1 and R_2 attached to the silicon atom, it is possible to modify and adjust the chemical and thermal stability, solubility, as well as electronic, optical, and rheological properties of the polymer (MALLMANN, M. D., 2020; ACOSTA, 2019; COLOMBO et al., 2010).

Figure 4 – Generic representation of organosilicon molecular structure.

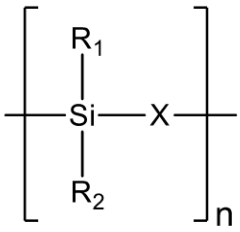

Source: Adapted from COLOMBO et al. (2010).

One of the key characteristics of PDC is the polymeric nature of their preceramic precursors. This property is crucial as it enables the polymers to exhibit adjustable solubility, meltability, and viscosity, making them amenable to various shaping techniques for the preparation of diverse ceramic shapes. These shapes include ceramic fibers, coatings, porous ceramics, ceramic microparts, dense monoliths, and, more recently, additive manufacturing parts (WEN et al., 2020; FU et al., 2019).

The diverse classes of silicon-based preceramic polymers are illustrated in Figure 5, showcasing the remarkable versatility of PDC in terms of their structures and corresponding physical-chemical characteristics (WEN et al., 2022; COLOMBO et al., 2010).

Figure 5 – Classes of silicon-based preceramic polymers.

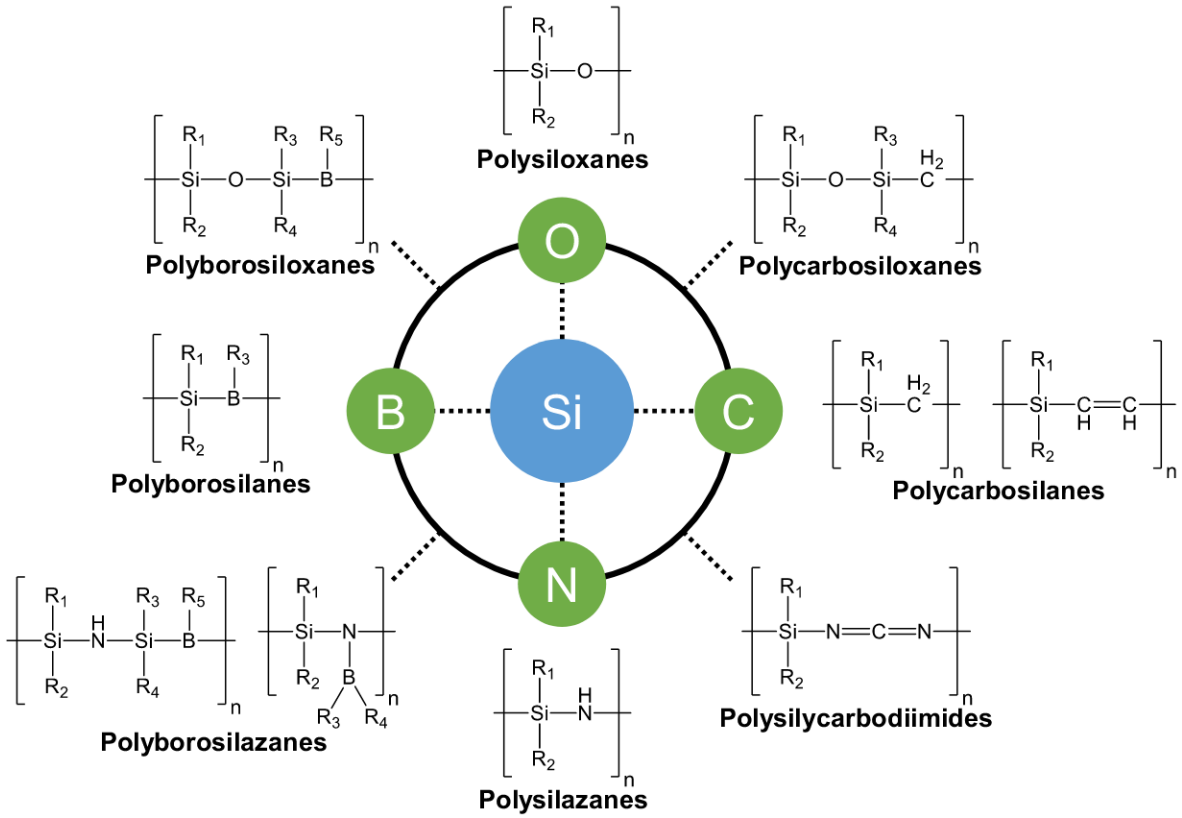

Source: Adapted from COLOMBO et al. (2010).

Because of this inherent versatility, PDC offer numerous advantages, including a favorable combination of high strength, exceptional hardness, excellent oxidation

resistance, as well as thermal stability and chemical durability. What sets PDC apart is their capacity to tailor and optimize properties through modifications in the chemical and phase composition, as well as the microstructure during synthesis and polymerization. The thermal treatment of PDC offers another advantage compared to conventional ceramic processing, primarily due to its requirement for significantly lower temperatures (CHAUDHARY et al., 2022; BARROSO, G. S. et al., 2015; COLOMBO et al., 2010).

The ultimate structures achieved from silicon-based polymers are notably shaped by several key factors. These factors encompass the chemistry and architecture of the precursors, the selected processing route, and the specific parameters applied during pyrolysis, including variables like heating rate, dwell time and atmosphere (that plays significant influence over the ceramic yield, alongside the chemical and phase composition of the resultant materials). A visual representation of the polymer-to-ceramic transformation concerning temperature can be observed in Figure 6. The PDC route includes both polymerization and shaping, which may involve complex forms, conducted at moderate temperatures of up to 400 °C. Subsequent to this, pyrolysis ensues at temperatures approaching 1400 °C, resulting in the creation of an amorphous ceramic. Notably, polycarbosilanes and polysilazanes undergo transformation into amorphous SiC and SiN or Si_3N_4 ceramics, respectively, during this process. Finally, an annealing phase follows at elevated temperatures, reaching up to 2000 °C, inducing the crystallization of the ceramic (ACKLEY et al., 2023; WEN et al., 2022; CHAUDHARY et al., 2022; MERA et al., 2015).

Figure 6 – Polymer-to-ceramic transformation with temperature increase.

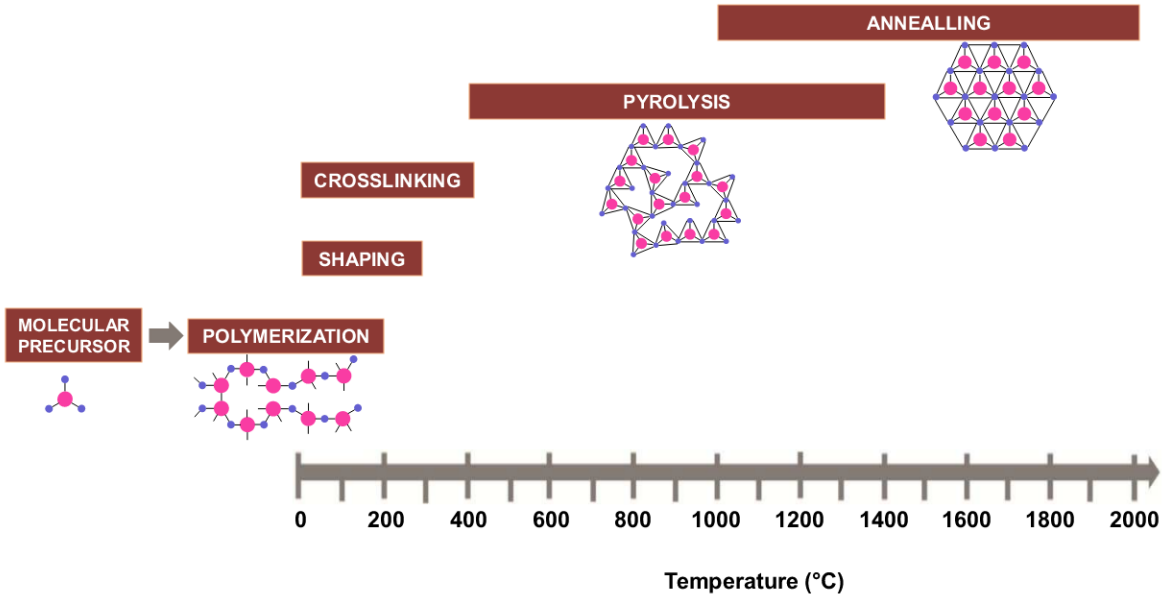

Source: Adapted from Mera et al. (2015).

A range of diverse silicon-based ceramics can be meticulously manufactured, with their compositions finely tuned by utilizing varied organosilicon preceramic polymers. This strategic approach yields non-oxide ceramics, exemplified by materials like silicon carbide, silicon nitride, as well as carbides, borides, and nitrides, often referred to as ultra-high-temperature ceramics. These ceramics serve a multitude of purposes in environments characterized by high temperatures and/or harsh conditions, making them immensely attractive. Notably, ceramics like SiC and Si_3N_4 demonstrate exceptional

efficacy within a subset of these demanding conditions, operational at temperatures reaching up to 1650 ℃ (ACKLEY et al., 2023; FU et al., 2019).

From the abundance of ceramic precursors available, three were specifically chosen for utilization in this research: Allylhydridopolycarbosilane (AHPCS), Perhydropolysilazane (PHPS), and Poly(methylvinyl)silazane (HTT). Subsequent sections will provide comprehensive details on each precursor, outlining their key characteristics and functionalities.

Silicon carbide was initially synthesized by Acheson (1893) through the fusion of silica sand and petroleum coke in a furnace operating at approximately 2300 ℃. Since this breakthrough, the Acheson process has stood as the cornerstone of industrial silicon carbide (SiC) production. Polycarbosilanes play a crucial role as extensively researched precursors for SiC, finding utility in applications such as electric and/or photo conductors, aerospace components, photoresist parts, and more (FU et al., 2019; ACHESON, 1893).

Renowned for their versatility, these compounds exhibit a striking diversity of compositional and property variations, both in their silicon backbone and side-chain groups. Multiple polycarbosilanes synthesis methods are available, including the Kumada rearrangement of polysilanes, also known as the Yajima process. Additional synthetic pathways include ring-opening polymerization, dehydrocoupling reaction of trimethylsilane and hydrosilylation of vinylhydridosilanes, among several others routes. Pyrolysis of polycarbosilanes within the temperature range of 800 ℃ and 1000 ℃ results in the formation of amorphous silicon carbide materials. This transformation involves the release of gases containing Si-H, Si-CH_3 and Si-CH_2-Si groups (ACKLEY et al., 2023; PRINT et al., 2023; ACOSTA, 2019; MERA et al., 2015; YAJIMA et al., 1978).

AHPCS is a good example of a widely used polycarbosilane and its molecular structure can be observed in Figure 7a. AHPCS is a clear, amber-colored, viscous liquid, and has been used as the matrix for ceramic compounds due to, among other characteristics, its relative stability in air, being liquid at room temperature and its low viscosity. The selection of AHPCS precursor is interesting the functional allyl group, that favors reaction mechanisms and improve its solubility and processability (PRINT et al., 2023; ACKLEY et al., 2023; ACOSTA, 2019).

The molecular structure of AHPCS indicates that two main mechanisms can contribute to its thermal cross-linking process, which are hydrosilylation and dehydrocoupling reactions as showed in Equations 2 and 3, respectively (ACKLEY et al., 2023; KAUR, A. et al., 2019).

$$\equiv Si–CH_2–CH{=}CH_2 + \equiv Si–H \rightarrow \equiv Si–CH_2–CH_2–CH_2–Si\equiv \tag{2}$$

$$\equiv Si–H + H–Si\equiv \rightarrow \equiv Si–Si\equiv + H_2 \tag{3}$$

Cross-linking in AHPCS is believed to commence at approximately 160 ℃, initiated by the allyl groups through radical reactions, in addition to that mentioned in equations 2 and 3. These reactions lead to the formation of a moderately cross-linked polymer. Further cross-linking is speculated to take place through the homolytic scission of Si–H bonds, followed by the combination of the generated Si radicals (PRINT et al., 2023; ACKLEY et al., 2023).

Figure 7 – Molecular structures of the selected preceramic polymers.

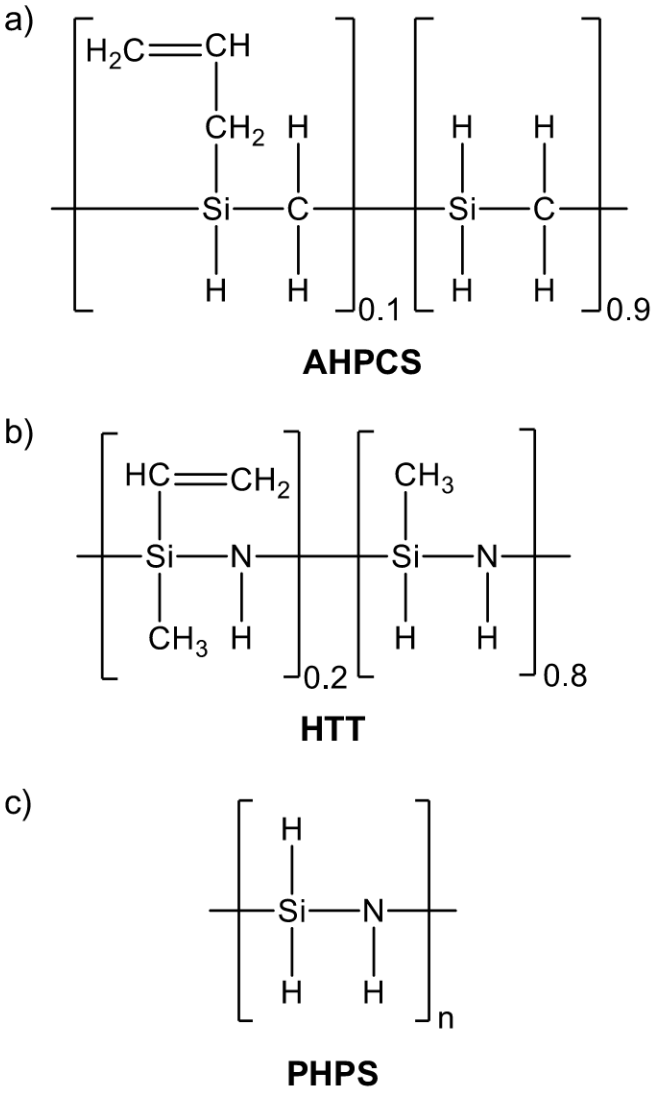

Source: Author (2023).

Silicon nitride holds significant industrial importance alongside silicon carbide as a promising material. Polysilazanes constitute another vital category of preceramic polymers utilized as precursors for silicon nitride production. A crucial nomenclature differentiation must be mentioned: when addressing amorphous ceramic silicon nitride, it is referred to as SiN, while Si_3N_4 is the preferred term for discussing its crystalline ceramic form, encompassing both α and β phases (ACKLEY et al., 2023).

Among the examples of widely used polysilazanes, there are two that can be highlighted: HTT and PHPS. In Figure 7b, it is possible to observe the molecular structure of HTT, which is characterized by the presence of the one methyl and one vinyl group. In Figure 7c, it is possible to observe the molecular structure of PHPS, and its characteristic as a carbon-free precursor for silicon nitride.

Hydrosilylation reactions take place in polysilazanes featuring Si–H and vinyl substituents. This rapid process occurs at relatively low temperatures, typically between 100 and 120 °C, resulting in the formation of Si-C-Si and Si-C-C-Si units. These reactions contribute to enhance the polymeric network's strength since the Si–C and C–C bonds remain unaffected by thermal treatment. Consequently, these reactions

enable the attainment of higher ceramic yields and increased carbon contents in the final ceramic materials. Dehydrogenation of Si–H/N–H or Si–H/Si–H groups initiates at temperatures around 300 °C leading to the creation of Si-N and Si-Si bonds, along with the release of hydrogen gas (MERA et al., 2015; COLOMBO et al., 2010).

Transamination processes are observed within the temperature range of 200 to 400 °C. These processes are accompanied by the release of amines, ammonia, or oligomeric silazanes, contributing to a reduction in nitrogen content during ceramic material pyrolysis. At moderate temperatures of 250 to 350 °C, vinyl polymerization occurs, leading to the creation of carbon chains. These chains may subsequently undergo a transformation into sp^2 carbon (also known as free carbon), without resulting in any mass loss. Additionally, the count of Si-N bonds in the ceramic materials increases with rising temperatures. This phenomenon is attributed to the interactions between Si–H and Si–CH_3 groups with N–H moieties (MERA et al., 2015; IONESCU et al., 2012).

The thermal processing of PHPS at 1000 °C under a nitrogen atmosphere results in a combination of both α and β-Si_3N_4 phases, along with silicon. However, when the PHPS is subjected to thermal treatment in an ammonia atmosphere, the creation of elemental silicon is inhibited. In the case of HTT, it is important to note that the presence of reactive organic segments, like vinyl group, although essential can influence the Si/C stoichiometry within the polymer, potentially leading to an excess of carbon content in the final PDC (ACKLEY et al., 2023; MALLMANN, M. et al., 2023; MALLMANN, M. D., 2020).

In the presence of catalysts, hydrosilylation can be significantly accelerated. Polysilazanes undergo an increased densification and cross-linking by the use of catalysts, such as Transition Metals (TM), since they are recognized for their catalytic capacity in activating these reactions at low temperatures (20 to 90 °C). Some studies have reported that in addition to catalyzing hydrosilylation reactions, transition metal chlorides also form metal nanoparticles. Therefore, the use of cobalt or nickel chloride can improve the crosslinking of the ceramic produced, as well as incorporate metallic particles within its structure (MALLMANN, M. et al., 2023; ACKLEY et al., 2023; ASAKUMA et al., 2022; TADA et al., 2021).

The strategic selection of three ceramic precursors from distinct classes aimed to assess the variations in the cobalt-doped ceramics produced. Additionally, it enabled the evaluation of their respective catalytic activities in the sodium borohydride hydrolysis reaction.

2.2.1 PDCs as catalyst supports

Since the catalytic activity is directly proportional to the number of active sites as well as their distribution in the structure, to improve the catalytic efficiency a widely used strategy is the use of metals in the form of nanoparticles as active sites. However, due to an increase in surface energy caused by the high number of surface atoms, nanoparticles tend to aggregate, inducing a loss in catalytic activity. In this sense, supports such as polymer-derived ceramics are a very interesting alternative because they can be modified in terms of composition, architecture and morphology in order to avoid such phenomena (LI, R. et al., 2022; LALE et al., 2020; BERNARD; MIELE, Philippe, 2014).

As active sites, the possibility of using TM (such as nickel, cobalt, copper and iron) instead of noble metals has been extensively explored, because they are more accessible, inexpensive and still efficient when comparing to noble metals. Among

the catalysts based on transition metals, those based on cobalt are very attractive due to their high activity for the hydrolysis as well as low cost (ERAT et al., 2022; ABDELHAMID, 2021; TADA et al., 2021; XIE, J.; XIE, Y., 2016).

Some strategies for incorporating TM in the ceramic matrix are reported in the literature. Generally, it can be broadly divided into two categories. One method is the addition of the TM after the shaping and crosslinking steps. This is not often reported, especially for mesoporous ceramics, most likely because there is a high possibility of low dispersion of metallic particles and pore blockage. Another method is to add the TM to the preceramic polymer with the aid of a solvent, and only then proceed with the shaping and crosslinking steps. Thus, the TM is more uniformly incorporated into the structure of the ceramic matrix, improving metal distribution and preventing agglomeration. Another advantage of the second method is to promote the *in-situ* growth of metal nanoparticles, making it a single-step process (ASAKUMA et al., 2022; TADA et al., 2021; LALE et al., 2018; ZAHEER et al., 2011).

The cobalt nucleation was already investigated by Tada et al. (2021), where a low-temperature *in-situ* formation of cobalt particles was firstly demonstrated, within a matrix of PHPS and cobalt (II) chloride. In this study, a proposed mechanism for the formation of cobalt crystals suggests a sequence of events. Within the temperature range of 220 to 350 °C, cobalt atoms coordinate with nitrogen atoms, resulting in the formation of Co_2N. Concurrently, chlorine atoms react both with hydrogen atoms (yielding HCl) and with silicon atoms from the ceramic precursor (resulting in SiH_xCl_y species). As the temperature rises within the range of 350 to 450 °C, the thermal decomposition of the pre-formed Co_2N takes place, ultimately leading to the nucleation of cobalt crystals (metallic). This suggested mechanism is highly plausible and accepted, providing a rationale for the formation of cobalt crystals within the amorphous ceramic matrix of PHPS. Furthermore, it may offer insights into the formation of such crystals within the matrices of other silazanes (such HTT) using $CoCl_2$ as a source of cobalt (TADA et al., 2021).

2.3 FINAL REMARKS ON THE LITERATURE REVIEW

The hydrolysis reaction of sodium borohydride not only holds significant importance in hydrogen (H_2) evolution, but it also provides an intriguing method to assess metal-doped ceramics synthesized through the PDC route. This is attributed to the harsh conditions involved, as depicted in Equation 1, leading to the formation of a strong base and exhibiting exothermic characteristics. Consequently, this reaction enables the evaluation of the material's chemical resistance, durability and robustness (LALE et al., 2020, 2018; AINGER; HERBERT, 1959).

In consideration of the preceding points, it becomes evident that H_2 is a pivotal topic facing the global energy landscape. A promising path for such generation lies in the utilization of the $NaBH_4$ hydrolysis reaction. Within this context, significant attention has been directed toward advanced catalyst supports for this reaction. However, they have not yet reached the required levels of efficiency necessary for large-scale application. In order to overcome this problem, many compounds have been investigated, with polymer-derived ceramics standing out in recent years due to their chemical stability and unique attributes.

Moreover, metal-doped polymer-derived ceramics have shown promising efficiency as catalysts for this application, specially those produced with cobalt. Therefore, this study is carried out with the objective of investigating hydrogen evolution through

the sodium borohydride hydrolysis reaction, employing cobalt-doped polymer-derived ceramics as catalyst. The primary aim is to mitigate the existing limitations, thus contributing to the development of catalysts that exhibit higher efficiency in releasing green hydrogen.

3 EXPERIMENTAL

This chapter is structured into four sections: Chemicals, Polymer-Derived Ceramics Synthesis, Characterization of Materials and Hydrolysis Reaction Tests. The first section provides a list of the reagents employed in the experimental procedures. The second section details the experimental procedures involved in the synthesis of cobalt-doped PDC. In the third section, the characterization techniques used in the produced materials are presented. Lastly, the fourth section is a description of the hydrolysis reaction tests and also the reusability tests of the catalysts produced. All the experimental procedures were carried out at the *Laboratório de Controle e Processos de Polimerização* (LCP), except for those explicitly mentioned. An overview of the experimental approach is presented in Figure 8.

Figure 8 – Experimental approach.

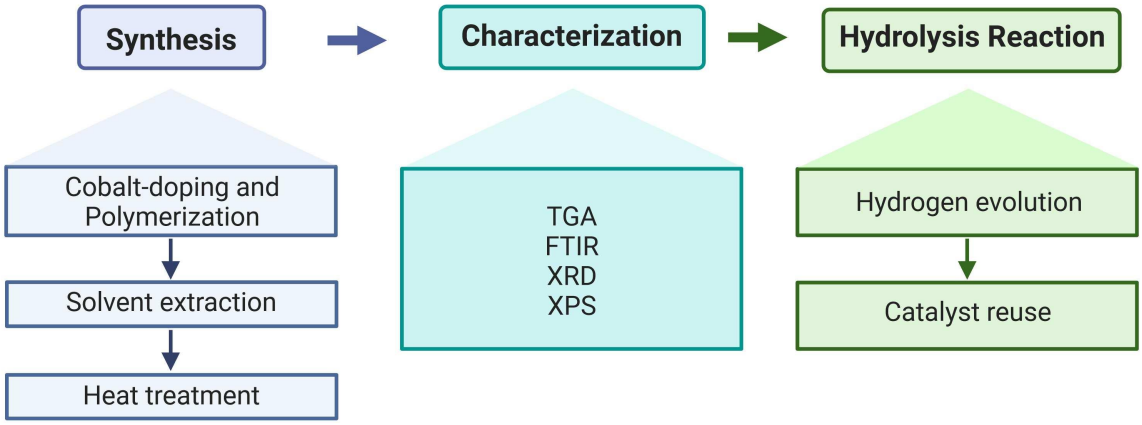

Source: Author (2023).

3.1 CHEMICALS

The reagents used in all preparations were purchased from commercial sources, without purification before using and are listed in Table 2.

Table 2 – Chemicals used in syntheses.

Chemical	Source
PHPS, 20 % vol in di-n-buthylether	durXtreme, Germany
HTT 1800	Merck Company, Germany
AHPCS	Starfire Systems, USA
Cobalt (II) chloride, anhydrous	Sigma-Aldrich, Germany
Toluene, 99.85%	Sigma-Aldrich, USA
Sodium Hydroxide, 98%	Qhemis, Brazil
Sodium Borohydride, 98%	Sigma-Aldrich, USA

Source: Author (2023).

3.2 POLYMER DERIVED CERAMICS SYNTHESIS

Prior to use, all glassware was kept in an oven at 60 ℃ overnight and removed only immediately before use. Also, glassware underwent a vacuum treatment for a minimum of 60 minutes to ensure the complete elimination of atmospheric air and humidity before adding the reagents, through a vacuum/argon line employing standard Schlenk techniques. The methodology for precursor synthesis was based on a recent publication of this group (MALLMANN, M. et al., 2023). The procedure started with the introduction of 50 mL of anhydrous toluene into a three-neck flask under an argon atmosphere. Next, 3 mL of the preceramic polymer (AHPCS, HTT or PHPS), were introduced into the system using a syringe. At this moment, magnetic stirring was activated in order to avoid decantation of the preceramic polymer. Following this, a calculated mass of cobalt(II) chloride ($CoCl_2$) as metallic precursor was added. $CoCl_2$ amount was precisely adjusted to attain a silicon:cobalt molar ratio of 2.5, considering the monomer as source of silicon to each calculation. The reaction was carried out under a controlled temperature and stirring conditions, maintaining an argon atmosphere and employing condensation by reflux, as illustrated in Figure 9.

Figure 9 – Schematic representation of reaction system.

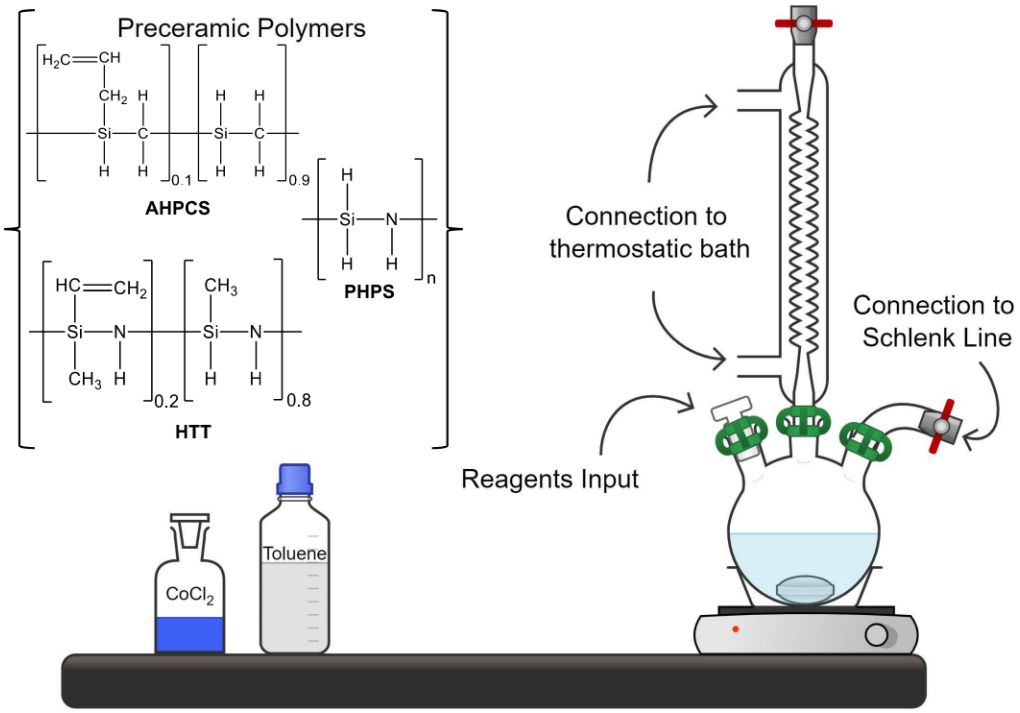

Source: Author (2023).

After adding the reagents, the system was stirred for 3 hours at room temperature, then heated up to 115 ℃ at a rate of 2 ℃ min^{-1}, remaining at this temperature for 15 hours. The selection of the reaction duration was based on prior investigations conducted by the research team. Various reaction times were experimentally tested, and the optimal outcome, with the most favorable final attributes, was observed at the 15-hour reaction (MALLMANN, M. D., 2020). During synthesis, the condenser temperature was maintained at 10℃ using a thermostatic bath. Then, the system was cooled down

to room temperature and opened under argon atmosphere to switch the condenser by the extraction system.

Solvent extraction was done by temperature and pressure difference. As showed in Figure 10, three-neck flask was heated up 115 ℃ after being coupled to a Schlenk flask which was submerged in liquid nitrogen. When subjected to temperature and pressure difference, the solvent was evaporated and conducted trough a distillation bridge to the Schlenk flask, where was frozen to further recovery. After about 3 hours of extraction, the metal-modified polymer was already in powder form.

Figure 10 – Schematic representation of solvent extraction system.

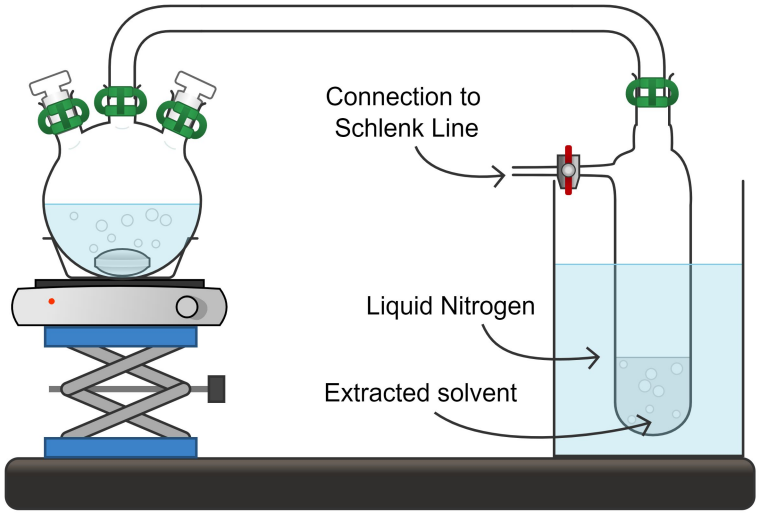

Source: Author (2023).

It is important to point out that the exact same synthesis procedure was used for the production of the three proposed materials. Another important point is the fact that in the synthesis using PHPS, a previous step was carried out, which is the extraction of di-n-buthylether solvent in which PHPS is stabilized. The preceramic polymer features 20% PHPS (v/v) in the commercial solution. This extraction was made using the same system represented earlier (Figure 10). For preceramic polymers HTT and AHPCS, this first extraction step was not necessary, as they are purchased without solvent and ready-to-use.

Finally, the powdered metal-modified polymers was submitted to the heat treatment. For that, the materials was transferred into an alumina vessel and placed within a tubular furnace for pyrolysis under an argon atmosphere to undergo polymer-to-ceramic transformation. The pyrolysis process was conducted at a controlled heating rate of 5 ℃ min^{-1}, progressing from room temperature to 1000 ℃ and a dwelling time of one hour at this temperature. After cooling, the cobalt-doped PDC catalysts were properly stored for further use.

Intermediate heat treatments were conducted to observe alterations in functional groups and the polymer-to-ceramics conversion (through Fourier-Transformed Infrared Spectroscopy (FTIR)) at three distinct temperatures: 200, 400, and 600 ℃. In this process, small portions of each sample were placed in alumina crucible under argon atmosphere and immediately positioned within the tubular furnace. Following the heat treatment and subsequent cooling, the sample was extracted, sealed in an argon-filled container, and immediately subjected to analysis. The entire analysis procedure was

meticulously planned to minimize the exposure time of the samples to air and humidity. This precaution was particularly emphasized given that, at lower heat treatment temperatures, the materials remained in the form of polymers, making it more susceptible to the influence of these environmental conditions.

It is crucial to emphasize that, as of now, there is no documentation in the literature detailing the development of ceramics from AHPCS doped with cobalt, making this material unprecedented.

3.3 CHARACTERIZATION OF MATERIALS

FTIR was employed to observe the changes in the functional groups of the compounds and the polymer-to-ceramic transformation, at three different pyrolysis temperatures: 200, 400, 600 °C, as well as in newly synthesized polymers. The analyzes were performed on an Agilent Technologies – Cary 660 Infrared Spectrophotometer, located at the Analysis Center of the Departament of Chemical Engineering (EQA), *Universidade Federal de Santa Catarina* (UFSC). Analyzes were performed by KBr pellets in a range of 4000-400 cm^{-1}.

Thermogravimetric Analysis (TGA) were used to determine the weight loss of the materials as the temperature increased. The analyzes were performed with 5 °C min^{-1} heating rate, up to 800 °C, under nitrogen atmosphere, at *Laboratório de Controle e Processos de Polimerização* (LCP) (EQA, UFSC) on a Netzsch STA 449 F3 Jupiter - Simultaneous Thermogravimetric Analyzer.

X-ray Diffraction Analysis (XRD) was utilized to determine the crystalline phase of the materials. The analyzes were performed on the *Laboratório Interdisciplinar para o Desenvolvimento de Nanoestruturas* (LINDEN) (EQA, UFSC), on a Rigaku MiniFlex 600 X-Ray Diffractometer, measuring in 2θ = 10 to 90°. The diffraction files were studied with the database from International Center for Diffraction Data (ICDD) Powder Diffraction File (PDF4).

XPS, was employed to investigate the surface and chemical state of the species. Data were acquired at LNNano- *Centro Nacional de Pesquisa em Energia e Materiais* (CNPEM), employing a Thermo Scientific Kα X-ray photoelectron spectrometer, using an Al Kα (1486.6 eV) radiation and a voltage in the X-ray tube of 12 kV. The measurements were performed in the: Survey, Co 2p, Si 2p, C 1s regions. The XPS data were analyzed using the Thermo Avantage software and Origin. For spectra calibration to mitigate surface-charging effects, the binding energy (BE) of the core level C 1s was set at 284.8 eV.

3.4 HYDROGEN EVOLUTION FROM HYDROLYSIS REACTION

To assess the produced ceramic materials, the sodium borohydride hydrolysis reaction was employed by using the water displacement method as the means to measure the volume of hydrogen generated. In this method, 10.0 mL of deionized water, 0.500 g of NaOH, 0.150 g of $NaBH_4$ and 0.100 g of the produced catalyst were introduced into the round-bottom flask, which was immediately closed, as hydrogen generation starts instantly. Figure 11 illustrates a generic setup for the system.

Figure 11 – Water displacement method system.

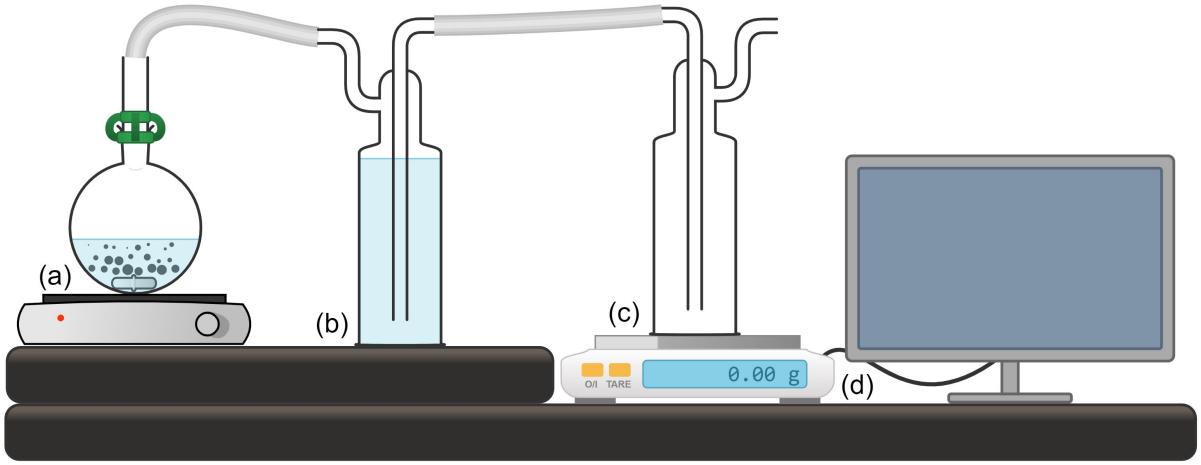

Source: Author (2023).

In this setup, (a) represents a round-bottom flask containing all reagents. Flask (b) represents the water displacement device itself, where the hydrogen gas generated in (a) displaces the water from flask (b) into the empty flask (c). The digital balance (d) was used to measure the overall mass and automatically records it in a computer software linked to the balance.

The mass of displaced water is equivalent to the volume of hydrogen generated in the hydrolysis of sodium borohydride. With the volume data as a function of time and concentrations used, it was possible to calculate both the hydrogen generation rate (HGR), the remaining concentration of $NaBH_4$ and consequently, the percentage conversion of $NaBH_4$ into H_2. Hydrolysis tests were carried out at four different temperatures (25, 40, 60 and 80 ℃), always using the same amounts of reagents and the same measurement system.

Finally, the catalyst that presented the highest HGR was submitted to reusability tests, which were divided in two different methods: by continuous use and washing procedure. For the first method, since the system did not detect any further variation in the amount of H_2 during the first use, flask (a) was opened and new loads of same amount of NaOH and $NaBH_4$ were added, along with 5 mL of deionized water. This process was done successive times until a decrease in the conversion values was detected. For the second method, after conversion decrease, the catalyst was washed by use of the following steps: addition of deionized water, manual agitation, centrifugation at 3000 rpm for 1 minute and removal of supernatant with a pipette. Five cycles of washing and centrifuging were performed to then dry the catalyst in an oven at 80 ℃ for one hour. After that, dried catalyst was subjected again to the hydrolysis reaction, following the same procedure used before washing.

4 RESULTS AND DISCUSSION

In this chapter, the experimental results of characterization and evaluation of the materials catalytic activity in the hydrolysis of sodium borohydride are presented and discussed. It is divided into three main sections: Thermal Analysis, Chemical and Structural Characterization and lastly, Test on Hydrolysis Reaction. The obtained materials were assigned distinct nomenclatures based on their respective preceramic polymer and Silicon:Cobalt molar ratio (based on precursor's monomer), as outlined in Table 3. Therefore, from this point on, this nomenclature will be used to describe the results.

Table 3 – Nomenclature of obtained PDC.

Nomenclature	Preceramic polymer	Si:Co molar ratio	$CoCl_2$ mass (g)
HTCo2.5	HTT1800	2.5	2.51
AHCo2.5	AHPCS	2.5	3.24
PHCo2.5	PHPS	2.5	3.60

Source: Author (2023).

Following the synthesis process outlined in the preceding chapter and subsequent solvent extraction up to 115℃, the newly synthesized polymers (materials before heat treatment) exhibited a distinct blue color attributed to the presence of cobalt, irrespective of the chosen ceramic precursor. The visual appearance of the synthesized polymers can be observed in Figure 12.

Figure 12 – Visual aspect of synthesized polymers.

Source: Author (2023).

4.1 THERMAL ANALYSIS

To explore polymer-to-ceramic conversions, newly produced polymers were analyzed using TGA. The analysis results are shown in Figure 13, in which some significant mass losses can be observed. Graphs with DTG curves are presented in Appendix B for a clearer view.

Figure 13 – Thermogravimetric Analysis curves.

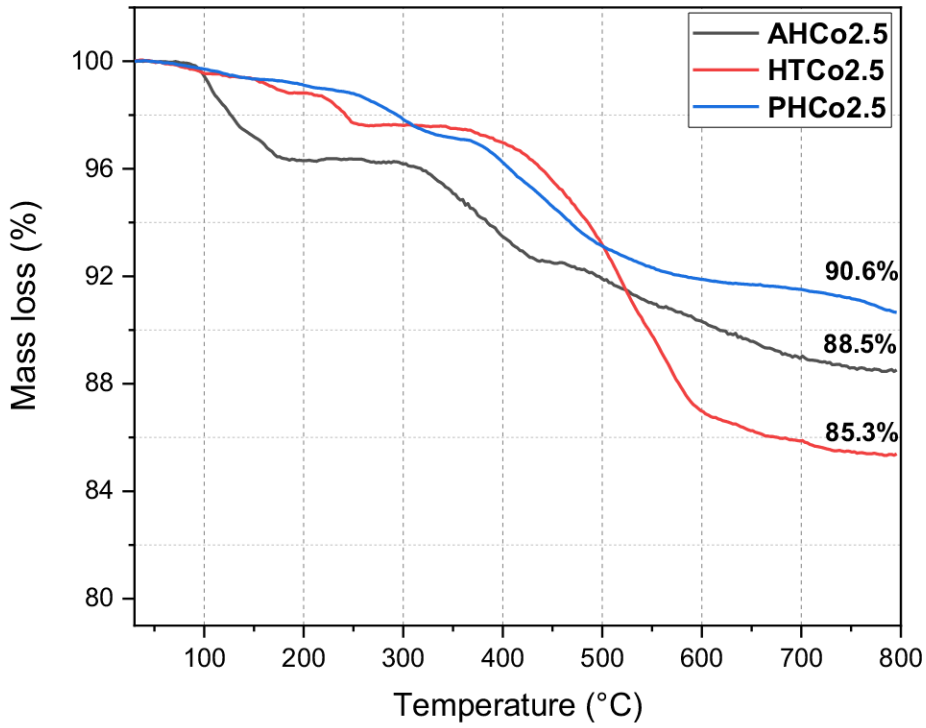

Source: Author (2023).

Initially for **AHCo2.5**, three losses were identified. The first one, at around 106 ℃, occur in the range where volatilization of the oligomers are described upon the initiation of cross-linking, although with a lower loss when compared to pure AHPCS reported in the literature (ACOSTA, 2019). This suggests that the cobalt doping did not prevent the oligomers volatilization, as happens with boron modified AHPCS, for example (SCHMIDT et al., 2017; ACOSTA, 2019). The second and third losses are found at around 305 ℃ and at around 456 ℃, and it can indicate the break of side groups bonds, with loss of volatile gases such as CH_3CH_3, SiH_4 and CH_3SiH_3 (from 300 to 500 ℃), as well as the start of dehydrocoupling reaction, releasing hydrogen. These losses are also smaller than those identified in pure AHPCS (ACOSTA, 2019). Another important information to be observed in the TGA curve is the obtained ceramic yield, of 88.51% for the cobalt-doped AHPCS, increased in relation to the pure AHPCS (around 70%) (SCHMIDT et al., 2017; ACOSTA, 2019; WANG, Q. et al., 2020; AL-AJRASH et al., 2021; YANG et al., 2022; PRINT et al., 2023).

HTCo2.5 curve shows mass losses in approximately 210 and 340 ℃, indicating the release of hydrocarbon oligomers. Also, a mass loss at around 500 ℃, are probably related to the release of hydrogen and methane gases, due to dehydrocoupling reactions. There was also a increase in **HTCo2.5** ceramic yield (85.35%) in comparison to pure HTT (about 68%) reported in the literature (LALE et al., 2016; MALLMANN, M. D., 2020; WANG, J. et al., 2020a, 2022a).

Finally, for **PHCo2.5**, it is possible to notice the highest ceramic yield of all three materials, that is, equal to 90.61%, greater than the reported for pure PHPS in the

literature, around 77% (MALLMANN, M. D., 2020). The mass losses observed for the material are found at approximately 250 and 350 °C. As reported in the literature, mass losses in this range may correspond to release of gaseous species, such as hydrochloric acid, monochlorosilane and dichlorosilane. Also, according to Tada et al. (2021), such losses may be related to the formation of metallic cobalt within the ceramic matrix (LALE et al., 2016; SMOKOVYCH et al., 2019; TADA et al., 2021; ZHAN et al., 2022).

In short, the results obtained with the thermogravimetric analyzes show once again the important role of cobalt in promoting higher crosslinking due to dehydrocoupling reaction and/or transamination reactions, consequently increasing ceramic yield, as observed for the three different precursors used (TADA et al., 2021; MALLMANN, M. et al., 2023; ACKLEY et al., 2023).

4.2 CHEMICAL AND STRUCTURAL CHARACTERIZATION

4.2.1 Fourier-Transformed Infrared Spectroscopy (FTIR)

The produced cobalt-doped polymers were subjected to FTIR analysis to comprehend the presence and variation of functional groups with increasing temperature.

For the cobalt-doped AHPCS, **AHCo2.5**, the changes in the spectrum according to temperature can be seen in Figure 14. The results obtained for **AHCo2.5** polymer show that before heat treatment, the spectrum presents the same main features observed for the spectrum of pure AHPCS found in literature, indicating the AHPCS silicon backbone in the produced material (AL-AJRASH et al., 2021; WANG, Q. et al., 2020; ACOSTA, 2019; RAHMAN et al., 2014). The presence of a band in the region of 750 cm^{-1} is attributed to the bending vibration (δ) of the Si-CH_3 bond, while at 2100 cm^{-1}, to the stretching vibration (ν) of the Si-H bond (YANG et al., 2022; ACOSTA, 2019). Bands at 1351 and 2900 cm^{-1} correspond to stretching C–H in Si–CH- bonds, and stretching of C=C bond in molecules may be indicated by the band at 1630 cm^{-1} (double bond of the allyl group) (PRINT et al., 2023). Furthermore, bands at 1250, 1037 and 940 cm^{-1} were attributed to Si–CH_3 stretching, CH_2 bending in Si-CH_2-Si bond and Si–H bending vibration, respectively (YANG et al., 2022). The band at around 3400 cm^{-1} is probably due to water adsorbed by the potassium bromide during FTIR testing (WANG, Q. et al., 2020; RAHMAN et al., 2014).

It is possible to note that with the temperature increase, all described bands decrease in intensity, with exception of the band at 1037 cm^{-1}, which still presents a strong signal even at 600 °C, confirming that the final structure remains with the AHPCS silicon backbone. Additionally, the decrease in intensity of the bands as the temperature increases occur probably due to crosslinking reactions occurring with increasing temperature, via dehydrocoupling reactions and to decomposition of the organic groups (RAHMAN et al., 2014; ACOSTA, 2019; WANG, Q. et al., 2020; AL-AJRASH et al., 2021).

Figure 14 – FTIR spectrum of **AHCo2.5** at different temperatures.

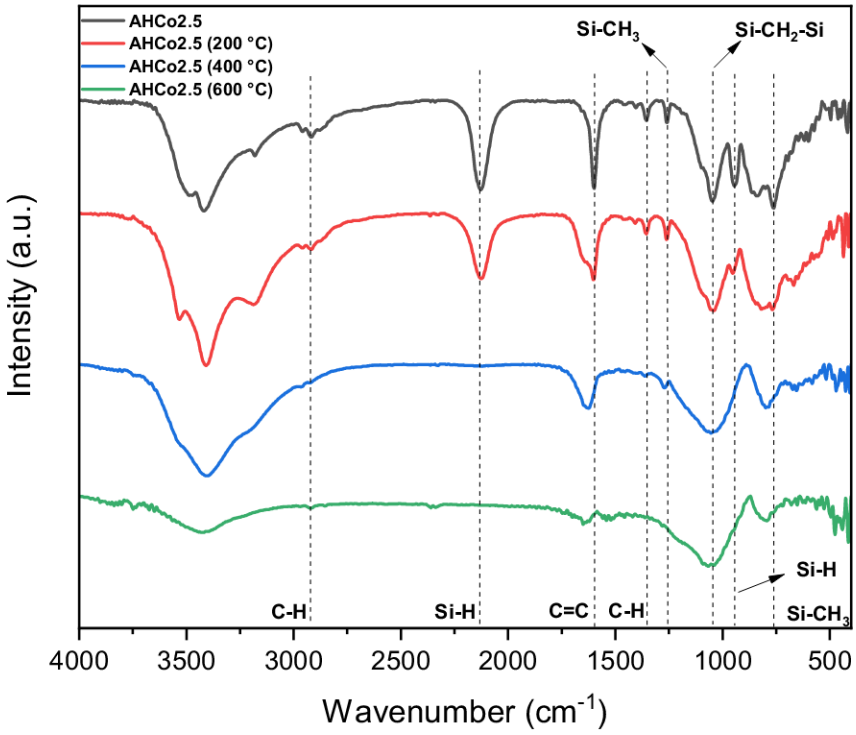

Source: Author (2023).

For the cobalt-doped HTT, **HTCo2.5**, the changes in the spectrum according to temperature can be seen in Figure 15. The main bands observed in the spectrum of the **HTCo2.5** polymer are characteristic for the functional groups present in pure HTT (MALLMANN, M. D., 2020). Bands at 3380 and 1160 cm^{-1} correspond to the N-H bond stretching vibration (ν) and to N-H bond bending (δ) on Si-NH-Si unit, respectively (FLORES et al., 2013; AWIN et al., 2023). In 2960 and 1590 cm^{-1}, bands are attributed to carbon functional group present in the preceramic polymer structure, as stretching of C-H bond and bending of C=C bond, respectively (WANG, J. et al., 2022a; MALLMANN, M. D., 2020). The Si-H stretching is attributed to the band at 2120 cm^{-1}, while the Si-C bonds of the HTT backbone may be observed at 1250 cm^{-1} indicating bending in Si-CH_3 bond and at 1400 cm^{-1} for bending in Si-CH=CH_2 bond (WANG, J. et al., 2022b; FERREIRA et al., 2023).

The spectra obtained for **HTCo2.5** samples after heat treatment (200, 400 and 600 ℃) indicate structural changes in the material with increasing temperature. It is noted that with the increase in temperature to which the **HTCo2.5** sample was subjected, almost all bands decrease in intensity, with the 3380 band almost disappearing completely, and 2960, 2120 and 1400 bands completely disappearing at 600 ℃. Furthermore, it is also possible to observe the appearance and increasing of the band related to Si-NH-Si bonds, at to around 1160 cm^{-1}, with increasing temperature. This behavior indicates that the crosslinking reactions are in fact occurring with the temperature increase, maintaining the HTT backbone (MALLMANN, M. D., 2020; WANG, J. et al., 2022b, 2022a; AWIN et al., 2023).

Figure 15 – FTIR spectrum of **HTCo2.5** at different temperatures.

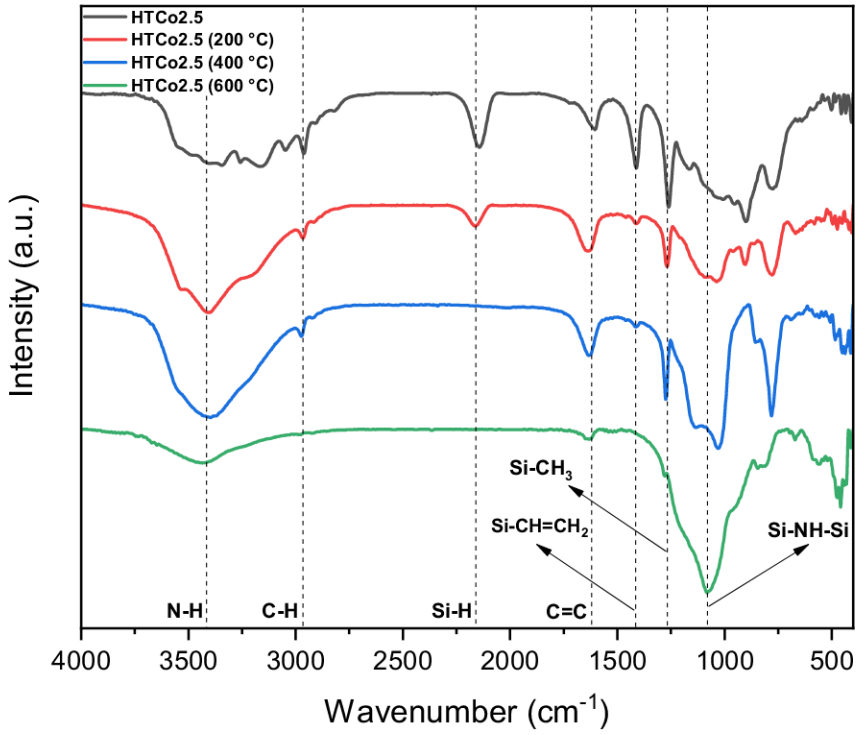

Source: Author (2023).

For the cobalt-doped PHPS, **PHCo2.5**, the changes in the spectrum according to temperature increase can be seen in Figure 16. Some characteristic bands of pure PHPS are also observed in the spectrum obtained for the polymer (ASAKUMA et al., 2022; CHEN, Q. et al., 2021; DUO et al., 2020). The spectrum of cobalt-doped PHPS polymer presents a wide band at around 3400 cm^{-1} corresponding to stretching (ν) mode of N-H bond, a band at 2150 cm^{-1} representing stretching Si-H bond, also at 1180 cm^{-1} corresponding to bending (δ) mode of N-H bond of Si-NH-Si unit, and lastly, a band at 820 cm^{-1} that corresponds to bending Si-N bond also of Si-NH-Si unit (WANG, W.-Y. et al., 2023; DUO et al., 2020). Besides that, a band in 1400 cm^{-1} correspond to bending C-H, probably due to some residue from the solvent, since the precursor polymer does not have carbon in its structure (MALLMANN, M. D., 2020). For the spectra of **PHCo2.5** in the different temperatures, the same bands are present but they decrease in intensity as the temperature increases. This must be related to the occurence of crosslinking reactions. Also, the increase at the band in 1167 cm^{-1}, may indicate forming of Si-NH-Si bonds, in accordance with the crosslinking indications mentioned above (MALLMANN, M. et al., 2023; MALLMANN, M. D., 2020).

Figure 16 – FTIR spectrum of **PHCo2.5** at different temperatures.

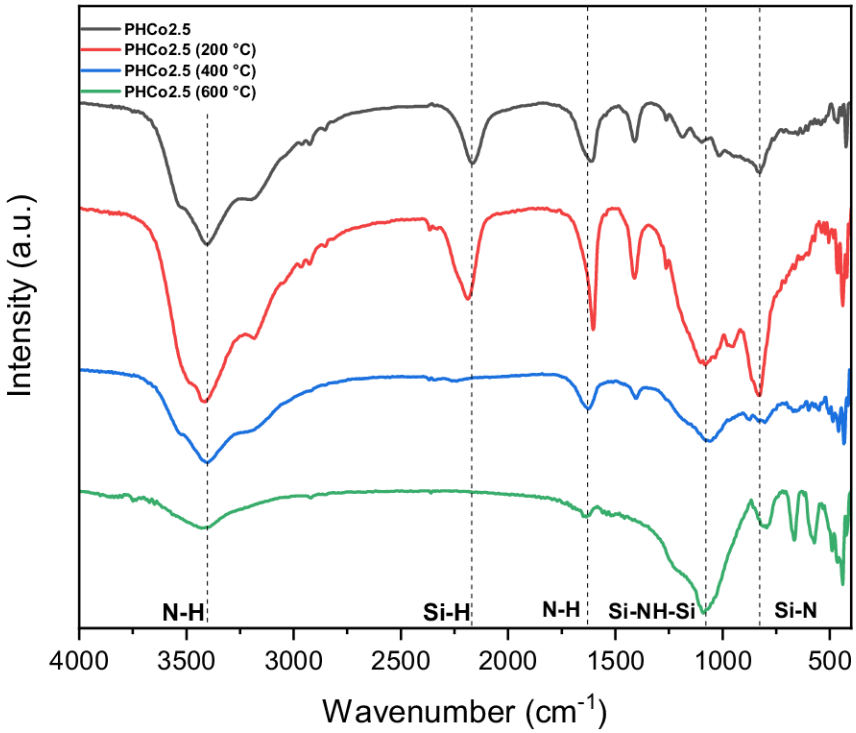

Source: Author (2023).

Observing the results obtained in the FTIR analysis, it can be stated that they are in agreement with those discussed in the TGA analysis (presented in section 4.1). With the mass losses observed between 200 and 600 ℃, there was also a decrease in the intensity of the bands corresponding to the bonds in CH_3-CH_3, SiH_4 and CH_3-SiH_3 species in **AHCo2.5**. Also, mass losses in in the same temperature range, are correlated to the already detected decrease in signal intensity related to the N-H and Si-H bonds of **HTCo2.5**. Furthermore, the mass losses in the range of 200 to 600 ℃ are in agreement with the decrease in intensity previously observed for the signal referring to the N-H, Si-N and Si-H bond s of **PHCo2.5**. These results confirm the occurrence of crosslinking reactions with release of correspondent compounds, and indicate the beginning of materials ceramization.

4.2.2 X-ray Diffraction (XRD)

To investigate the formation of crystalline phases in the ceramics produced, XRD was carried out.

For **AHCo2.5** the obtained diffractogram can be observed in the gray line in Figure 17. Signals at 2θ= 44.2158 °, 51.5225° and 76.1378°, correspond to cobalt in cubic crystal phase (β-Co)(ICDD file nº: 01-089-4307). Also, signals at 2θ= 28.4040°, 34.9703°, 40.5335°, 45.7136°, 50.2553°, 70.3374° and 80.9347°, correspond to cobalt monosilicide (CoSi) in cubic phase (ICDD file nº: 01-072-1328) (PRINT et al., 2023; ACOSTA, 2019; KAUR, S. et al., 2014). No peaks related to silicon carbide were identified. This was already expected and is explained by data reported in the literature, that the presence of amorphous SiC begins to be noticed in the system with heat treatments between 850 and 1200 ℃, and crystalline SiC at temperatures between 1250 and 1700 ℃ (PRINT et al., 2023; ACKLEY et al., 2023; BARROSO, G. et al., 2019). Since the

heat treatment of AHPCS was carried out up to 1000 ℃, for the presence of SiC to be present, the material must have been treated at temperatures greater than 1000 ℃.

Figure 17 – Diffractogram obtained for the three produced ceramic materials.

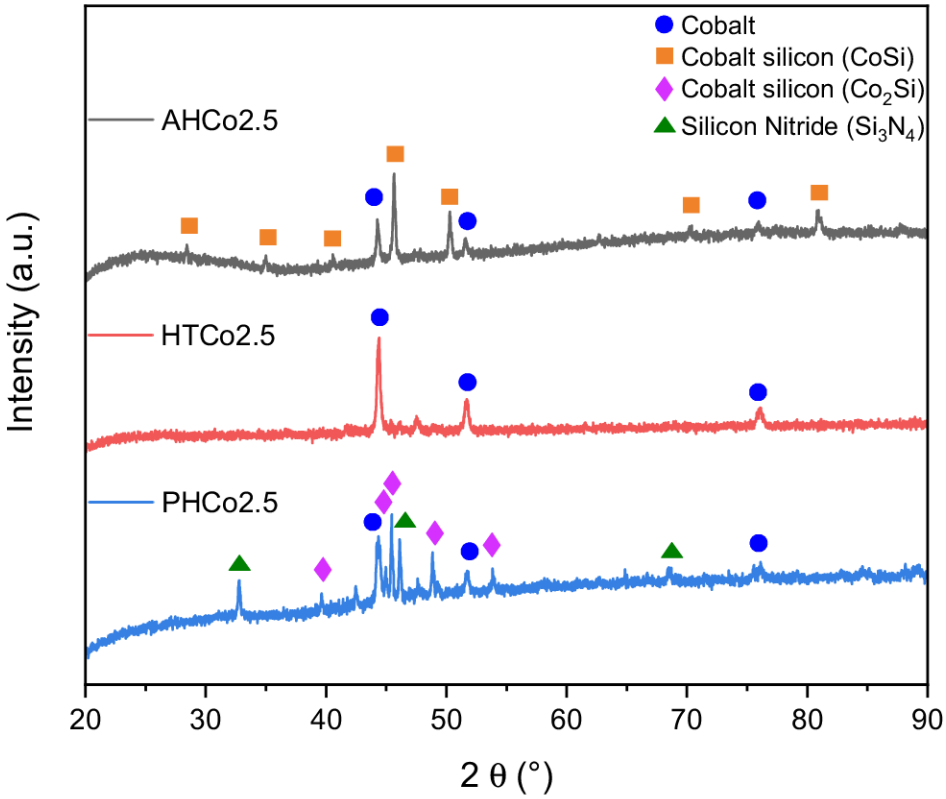

Source: Author (2023).

For **HTCo2.5** the obtained diffractogram can be observed in the red line in Figure 17. Signals at 2θ= 44.2158°, 51.5225° and 76.1378°, correspond to cobalt in cubic crystal (β-Co) (ICDD file nº: 01-089-4307). Also, there is a peak at 2θ= 47.594° that corresponds to cobalt in hexagonal crystal (α-Co) (ICDD file nº: 01-089-4308). This result agrees with what is expected for cobalt-doped derived from HTT, and heat treated at low temperatures. As recently reported in the literature, only the peaks referring to the growth of α and β-cobalt crystals are observed by XRD with the heat treatment up to 1000 ℃ (MALLMANN, M. et al., 2023; TADA et al., 2021; MANJUNATHA et al., 2019).

For **PHCo2.5** the obtained diffractogram can be observed in the blue line in Figure 17. Signals at 2θ= 44.2158°, 51.5225° and 76.1378°, correspond to cobalt in cubic crystal (β-Co) (ICDD file nº: 01-089-4307). Besides that, peaks appear at 2θ = 45.934°, 48.807°, 53.787° and are related to dicobalt silicide (Co_2Si) phase (ICDD file nº: 04-003-2126). Lastly, peaks at 2θ = 32.688° and 45.328° are associated to cobalt monosilicide (CoSi) in cubic phase (ICDD file nº: 01-072-1328) (MALLMANN, M. et al., 2023; TADA et al., 2021; MALLMANN, M. D., 2020).

The formation of cobalt silicide species (CoSi, Co_2Si) is probably due to a direct reaction between the silicon centers of the precursors and the cobalt atoms of $CoCl_2$ in the range between 700 and 800 ℃, and this formation has been previously reported in materials produced with polysilazanes and cobalt precursors. (WANG, J. et al., 2020b; MALLMANN, M. et al., 2023). This formation follows the reaction presented in Equation

4, as already reported for the synthesis of metal silicides, including cobalt ones by using microwave irradiation (CHEN, X.; LIANG, 2019; ZHANG et al., 2014).

$$2\,CoCl_{2(s)} + (2\,x + 1)\,Si_{(s)} \rightarrow 2\,CoSi_{x(s)} + SiCl_{4(g)} \quad (4)$$

Also, as CoSi is a metastable phase, it combines to silicon to further generate $CoSi_2$, and still, cobalt (II) chloride can combine with silicon to form Co_2Si, as showed in Equation 5 (MALLMANN, M. et al., 2023; ZHANG et al., 2014).

$$4\,CoCl_{2(s)} + 3\,Si_{(s)} \rightarrow 2\,Co_2Si_{(s)} + SiCl_{4(g)} \quad (5)$$

Metal silicides are a family of intermetallic compounds, composed of silicon and metal atoms, which can be in different proportions (ZHANG et al., 2019). Silicides formed with TM have interesting characteristics, such as high chemical resistance. Furthermore, TM-silicides have been reported to have a good activity to use in traditional heterogeneous catalytic reactions, such as hydrogenation, dehydrogenation and methanation, for example (ZHANG et al., 2018; CHEN, X.; LIANG, 2019).

According to the results obtained with XRD analysis, it is possible to confirm the *in-situ* growth of cobalt crystals within the amorphous ceramic matrix, as already reported in the literature recently. To find out if the formation of cobalt crystals took place on a nanometric scale, further studies and crystallite size analysis are necessary, which were not carried out in this work (TADA et al., 2021; MALLMANN, M. et al., 2023).

4.2.3 X-ray Photoelectron Spectroscopy

The materials prepared by heat treatment of **HTCo2.5**, **PHCo2.5**, and **AHCo2.5** at 1000 ℃ were subjected to XPS analysis. The Co2p, C1s, and Si2p spectra are presented in Figures 18, 19, and 20, respectively. The deconvoluted Co 2p envelope exhibited distinct behaviors for the analyzed materials, with the presence of Co^0 (778 and 793 eV) in **AHCo2.5** and in small quantities in **PHCo2.5**. According to Kim et al. (2008), these values represent the Co-Si bonding energies. The formation of Co-Si in both samples can also be observed in their respective diffractograms. CoSi, as previously reported in Anhua et al. (2014) and Kim et al. (2008), can be attributed to the reaction of cobalt metal with a SiCN/SiC matrix from ceramic precursors as the pyrolysis temperature increases. However, in contrast to the XRD analysis, **HTCo2.5** did not exhibit metallic cobalt in the XPS analysis, which may be due to material oxidation, as indicated by the formation of cobalt oxide in all the samples. The spectra exhibited a good fit, displaying two doublets: a $Co2p_{3/2}$ peak at 782 eV, a $Co2p_{1/2}$ peak at 798 eV, along with their corresponding satellite structures in approximately 788.3 and 804 eV, respectively, across all samples (LUO et al., 2021; SMYRNIOTI; IOANNIDES, 2017). These characteristics suggest of Co bonding in cobalt oxide, which was not present in the XRD results but is expected to develop over time as oxides form on the exposed sample surfaces.

Figure 18 – XPS Co2p spectra for a) **HTCo2.5**, b) **PHCo2.5** and c) **AHCo2.5**.

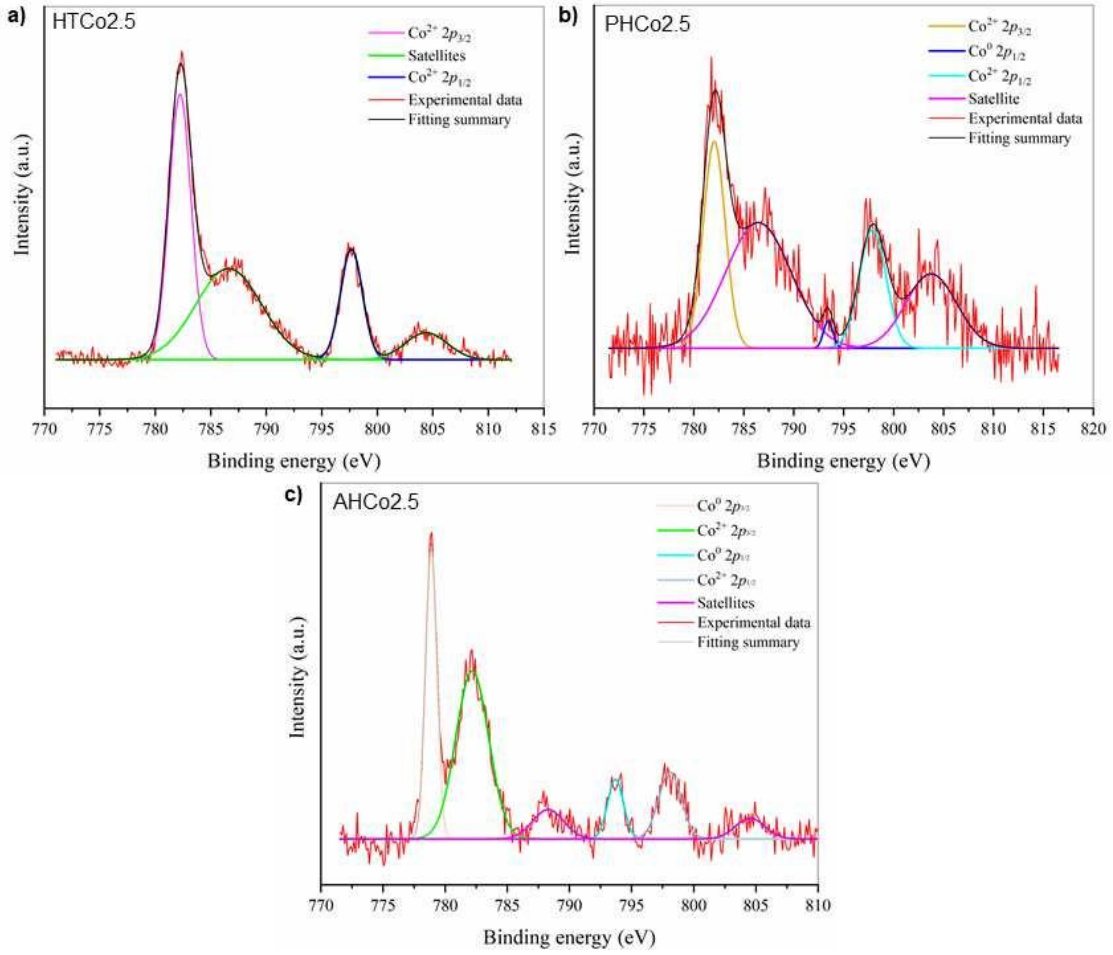

Source: Author (2023).

XPS survey spectra are presented in Appendix A and from its data, the surface atomic percentages of the three materials were obtained, as shown in Table 4.

Analyzing the composition of the samples based on their atomic percentages (Table 4), it was observed that the **HTCo2.5** had the highest cobalt content (%at). However, it exhibited the lowest catalytic activity at 353 K (922.14 mL min^{-1} $g_{cat}{}^{-1}$). In contrast, samples with lower %at. of Co showed higher catalytic activity at the same temperature. Notably, the **PHCo2.5** (HGR of 7,641.42 mL min^{-1} $g_{cat}{}^{-1}$) with only 0.48 %at. of Co and the **AHCo2.5** (HGR of 3,969.13 mL min^{-1} $g_{cat}{}^{-1}$) with 1.1 %at. of Co demonstrated enhanced catalytic activity. The Hydrogen Generation Rate may be influenced by various conditions and warrants further investigation, including factors related to matrix crystallization, the presence of silicides, carbon content, and other parameters.

Table 4 – Atomic concentration of synthetized materials by XPS.

	Surface Atomic concentration (%)						
Material	**C1s**	**O1s**	**Si2p**	**Si2s**	**Cl2p**	**Co2p**	**N1s**
AHCo2.5	53.28	19.61	12.01	11.87	2.13	1.11	-
HTCo2.5	16.36	31.94	17.50	16.46	5.67	2.68	9.40
PHCo2.5	10.46	44.30	21.15	22.82	0.32	0.48	0.46

Source: Author (2023).

Moreover, the carbon contribution within the specimens was investigated, as depicted in Figure 19 the outcomes derived from the deconvolution analysis of the C1s peak in the materials. The high-intensity peak in green in all materials corresponds to the C-C bond (284.7) and can be associated to the presence of segregated carbon in the materials, probably due to the presence of free carbon nanodomains within the SiCN amorphous phase. The peak at approximately 285.5 eV in the samples suggests the presence of C–O bonding and is attributed to the presence of oxygen contamination at the surface. The **AHCo2.5** sample exhibits a peak at about 283.1 eV, which can be attributed to Si-C bonding (HANNIET, 2021; FENG, 2020; KAUR, S., 2016).

When examining the atomic percentage of carbon in **PHCo2.5**, it becomes intriguing to note an approximate 11% presence of carbon. This is noteworthy, given the inherent characteristic of PHPS not typically containing carbon atoms in its structure. The observed carbon percentage may be linked to the intentional addition of low-carbon molecules to the commercial PHPS to prevent reactions. Alternatively, it could be attributed to potential external contamination residues, especially given that XPS analysis focuses on surface-level examination.

Figure 19 – XPS C 1s spectra for a) **HTCo2.5**, b) **PHCo2.5** and c) **AHCo2.5**.

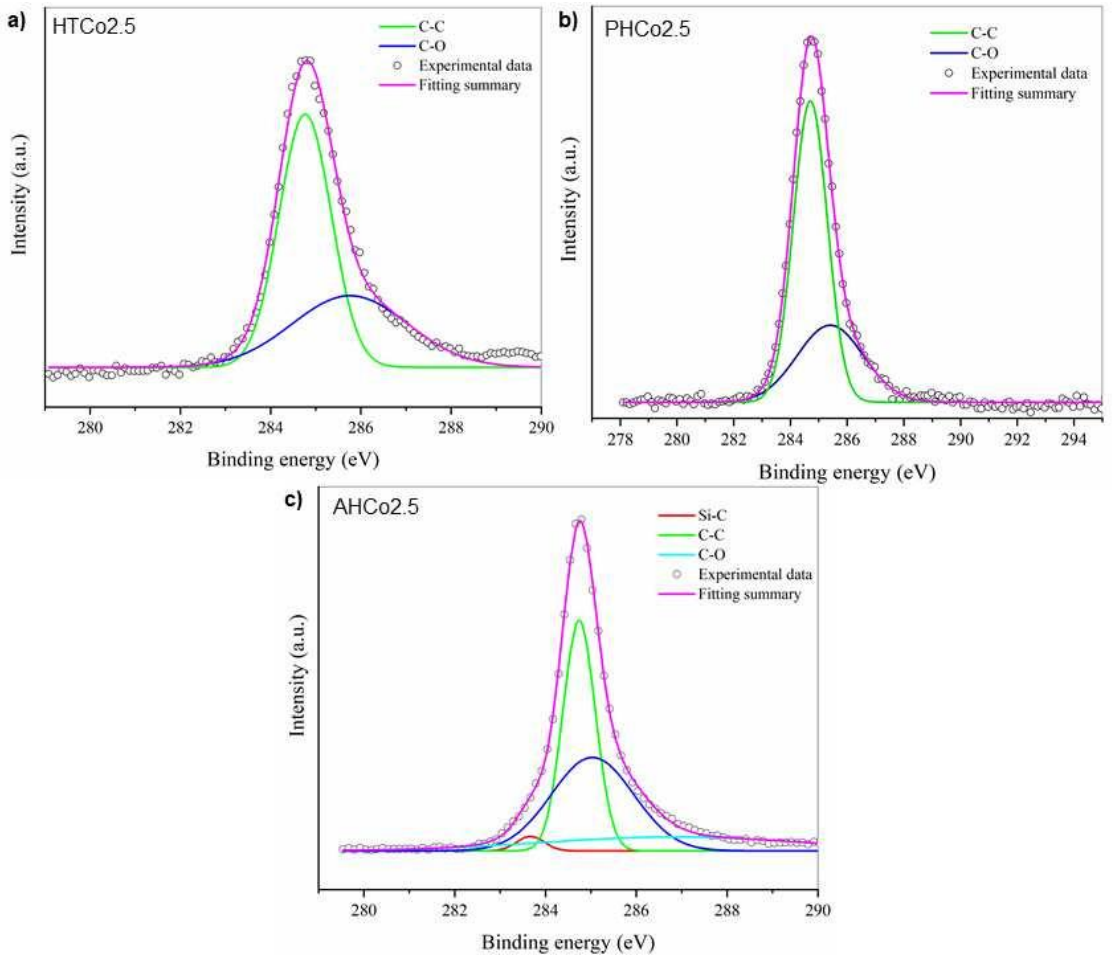

Source: Author (2023).

The deconvoluted Si2p spectrum in Figure 20 reveals a peak at 103.5 eV across all samples assigned to silica, thus demonstrating sample contamination. However, unique peaks were observed solely in the **AHCo2.5** sample at 101 eV, possibly corresponding to crystalline silicon carbide, while the signal at 101.6 eV was attributed to Si-C bonds in SiC(O) (HANNIET, 2021; FENG, 2020; KAUR, S., 2016).

Figure 20 – XPS Si2p spectra for a) **HTCo2.5**, b) **PHCo2.5** and c) **AHCo2.5**.

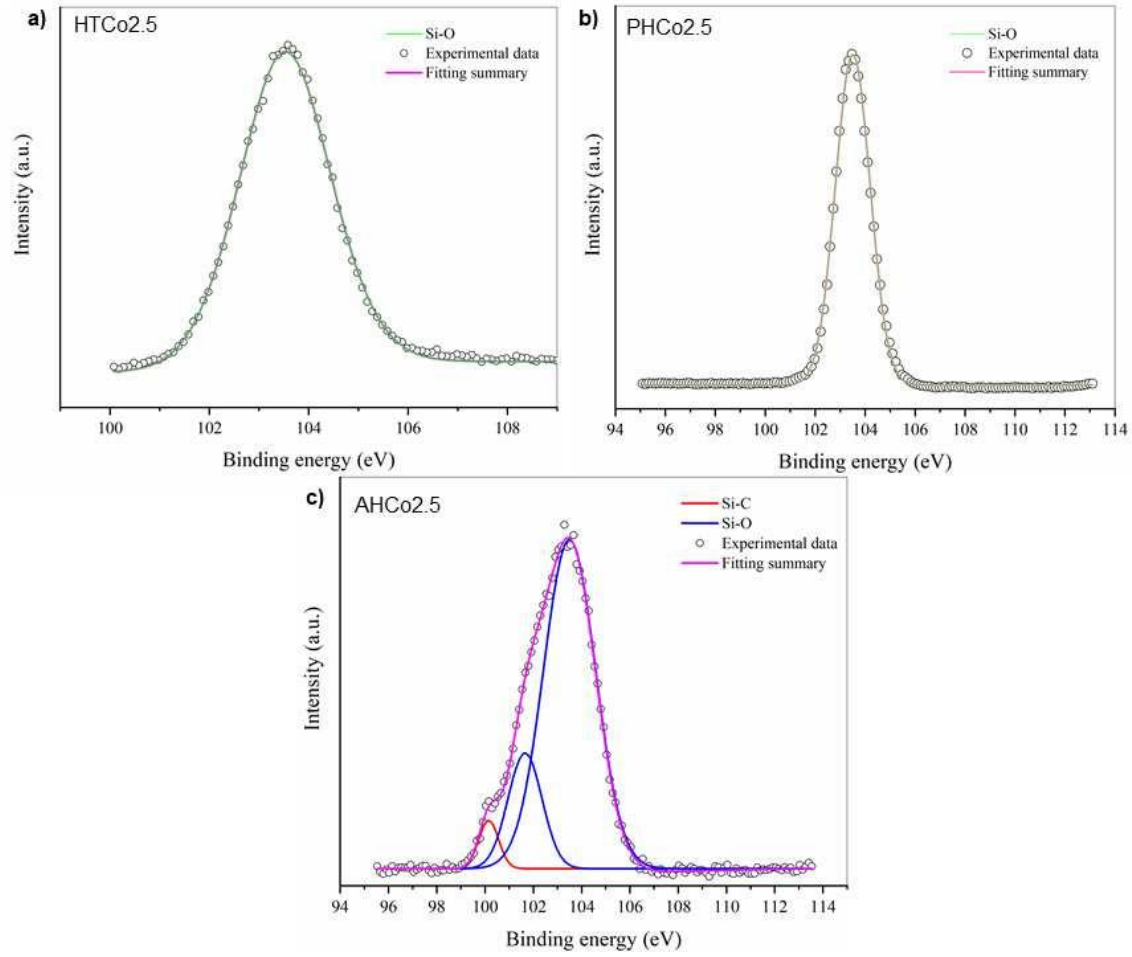

Source: Author (2023).

4.3 TESTS ON HYDROLYSIS REACTION

The difficulties of storing and transporting hydrogen are obstacles that can be overcome when using metal hydrides as storage materials. This makes $NaBH_4$ an excellent material in the energy transition scenario and makes its hydrolysis reaction extremely important. Furthermore, the catalytic hydrolysis of $NaBH_4$ produces pure hydrogen in a controlled manner (MAKIABADI et al., 2020; SONG et al., 2023). Apart from its significant role in the production of H_2, the sodium borohydride hydrolysis reaction serves as an intriguing method to evaluate metal-doped ceramics fabricated through the PDC route. This is attributed to the reaction's harsh conditions, as indicated by Equation 1, with the formation of a potent base ($NaB(OH)_4$) and its exothermic nature. Consequently, this reaction enables the assessment of the material's chemical resistance (LALE et al., 2018; ABDELHAMID, 2021).

For the tests of the produced materials, four different temperatures (298, 313, 333 and 353 K) was tested with the same amount of reagents, using the water displacement system previously presented (Figure 11, Chapter 3). Then, the total volume of hydrogen generated was recorded as a function of time and the total conversion of $NaBH_4$ into H_2 was calculated for each temperature. These results can be observed in terms of total hydrogen evolution (a) and conversion of $NaBH_4$ (b), in Figure 21 for **AHCo2.5**, in Figure 22 for **HTCo2.5** and in Figure 23 for **PHCo2.5**.

It can be noticed that for all three materials, both HGR and conversion increased as temperature also increased, although with a slightly different curve profile for each material. In addition, the highest sodium borohydride conversion values were obtained at the highest temperature tested (353 K), with the highest value being 99% for **AHCo2.5**, followed by **PHCo2.5** and **HTCo2.5** with 96% and 87%, respectively.

Figure 21 – H_2 volume generated (a) and conversion of $NaBH_4$ (b) for **AHCo2.5**.

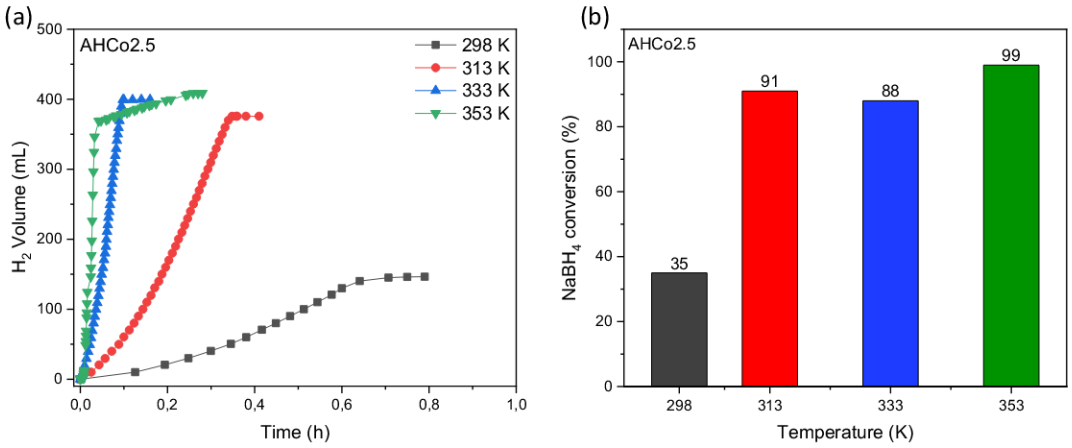

Source: Author (2023).

Figure 22 – H_2 volume generated (a) and conversion of $NaBH_4$ (b) for **HTCo2.5**.

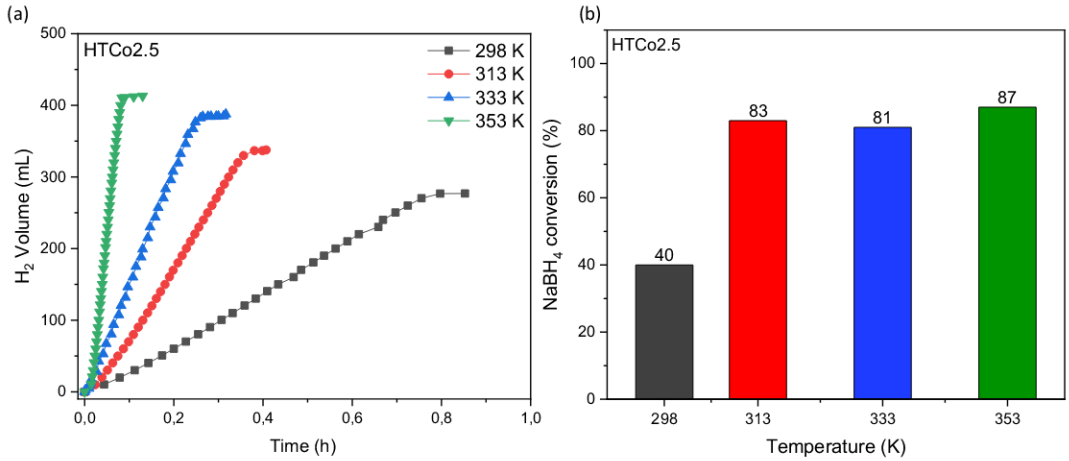

Source: Author (2023).

Figure 23 – H_2 volume generated (a) and conversion of $NaBH_4$ (b) for **PHCo2.5**.

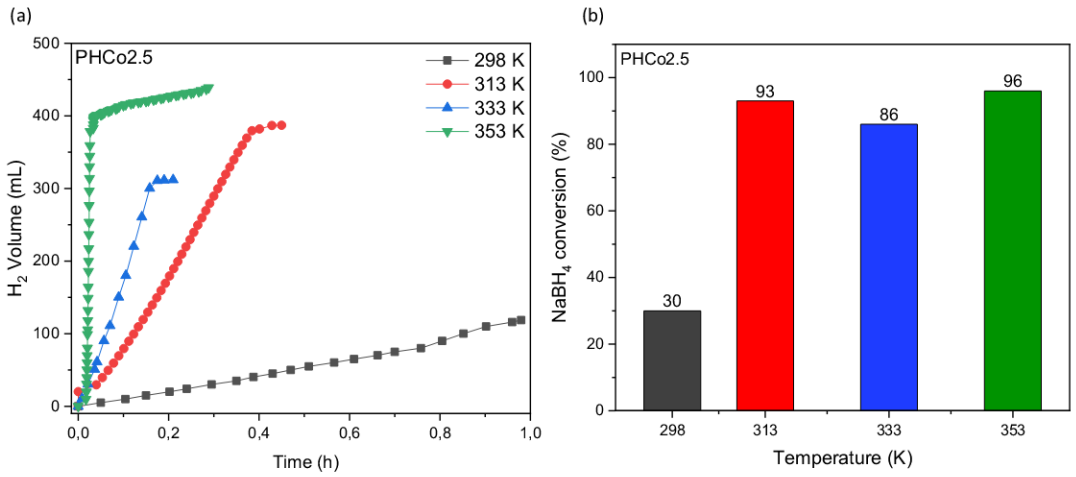

Source: Author (2023).

These results are in agreement with data from the literature, in which the volume of hydrogen produced tends to be greater as the temperature increases, in addition to a consequent increase in the Hydrogen Generation Rate (HGR), regardless the type of catalytic support used (UGALE et al., 2022; KYTSYA et al., 2022; ECER et al., 2023; SONG et al., 2023; HANSU, 2023).

An interesting fact is that for all three materials, in the lowest temperature (298 K), the conversion of $NaBH_4$ into H_2 was calculated as 40% or lower. This must be related to the solubility problem of both the reagents and products. Considering the lower solubility of the borates by-products when at lower temperatures, once precipitation occurs, catalysts sites are blocked, thus preventing hydrolysis with higher conversions. To avoid precipitation, higher temperatures can be adopted to increase solubility, or even use a diluted $NaBH_4$ solution (HUA et al., 2003; PINTO et al., 2006; SONG et al., 2023).

Typically, sodium hydroxide is introduced into the aqueous $NaBH_4$ solution to prevent self-hydrolysis, but this addition must be carefully calculated. As the NaOH concentration exceeds a certain value, hydrogen generation decreases due to the high alkalinity character of the solution. This increase in alkalinity results in a strong increase in the viscosity of the solution, strongly interfering with the reaction kinetics. In addition, the increase in the pH of the reaction medium leads to the precipitation of borates, due to their reduced solubility in basic media (KAUR, A. et al., 2019; RETNAMMA et al., 2011).

The hydrogen generation rate (HGR) was calculated in terms of mL min^{-1} $g_{cat}{}^{-1}$. For better visualization Table 5 shows HGR for all three materials as a function of temperature.

Table 5 – Hydrogen Generation Rate for the produced materials.

	HGR (mL min^{-1} $g_{cat}{}^{-1}$)		
T (K)	**AHCo2.5**	**HTCo2.5**	**PHCo2.5**
298	41.51	60.63	34.05
313	230.45	158.10	187.18
333	901.28	240.86	374.13
353	3,969.13	922.14	7,641.42

Source: Author (2023).

Some observations arise regarding the calculated HGR values. Firstly, there is a striking temperature-dependent relationship evident in the $NaBH_4$ hydrolysis reaction. This is particularly noticeable when comparing two different temperatures. The HGR values obtained at the temperature of 313 K are between 3 to 5 times greater than those obtained at 298 K. When further increasing the reaction temperature, the values obtained at 333 K are between 2 to 4 times greater than at 313 K, suggesting a considerable increase, but not as pronounced. However, when the comparison is made between 333 and 353 K, a much more significant increase is noted, with HGR values up to **20 times** higher for **PHCo2.5**.

Additionally, at the highest temperature tested (353 K), this significant increase in HGR values mirrors the trends previously discussed regarding $NaBH_4$ conversion rates. This behavior is observed in all three materials among which **PHCo2.5** stands out with the highest HGR value, reaching an impressive 7,641.42 mL min^{-1} $g_{cat}{}^{-1}$, as can be clearly seen in Figure 24.

Figure 24 – HGR for the produced materials, in graphic representation.

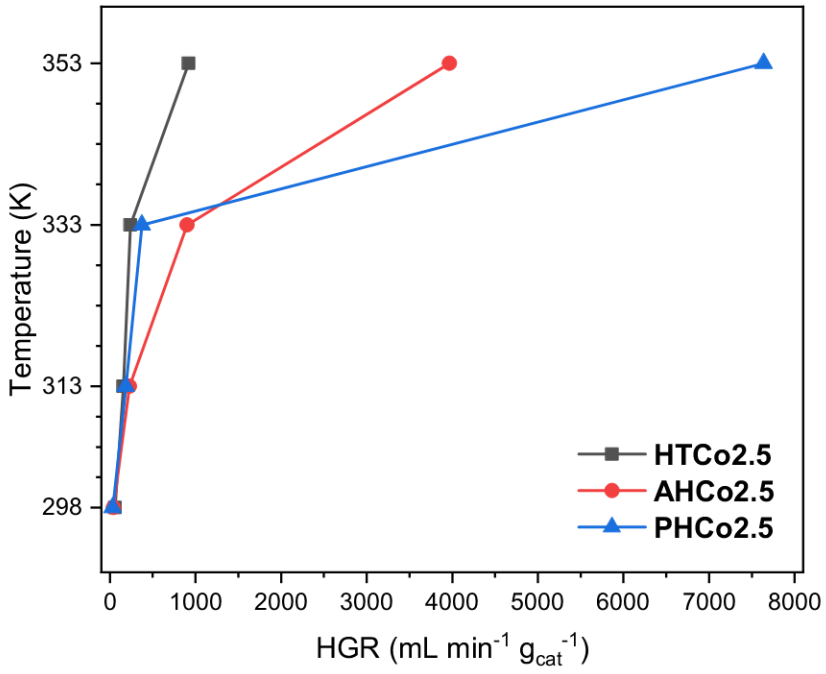

Source: Author (2023).

Analyzing the composition of the samples based on their atomic percentages (Table 4), it was observed that the **HTCo2.5** had the highest cobalt content (%at.) at the

surface. However, it exhibited the lowest catalytic activity at 353 K (922.14 mL min^{-1} $g_{cat}{}^{-1}$). In contrast, samples with lower %at. of Co showed higher catalytic activity at the same temperature. Notably, the **PHCo2.5** (HGR of 7,641.42 mL min^{-1} $g_{cat}{}^{-1}$) with only 0.48 %at. of Co at the surface and the **AHCo2.5** (HGR of 3,969.13 mL min^{-1} $g_{cat}{}^{-1}$) with 1.1 %at. of Co at the surface, demonstrated enhanced catalytic activity. The Hydrogen Generation Rate may be influenced by various conditions and warrants further investigation, including factors related to matrix crystallization, the presence of silicides, carbon content, and other parameters.

Cobalt silicide species probably have the role of improving the catalyst activity, increasing HGR values. This is because pure cobalt silicide species are reported as catalysts in hydrogenation and dehydrogenation reactions, with a growing number of publications in the past few years (ZHANG et al., 2019; CHEN, X.; LIANG, 2019; ZHANG et al., 2018).

This ability of silicides can be used to explain the catalytic activity of the materials produced in terms of HGR. For **HTCo2.5**, no cobalt silicides peaks were observed in the XRD analysis, this would indicate a reason why this material presented the most modest HGR values among the three.

In contrast, **AHCo2.5** and **PHCo2.5** presented peaks related to cobalt silicide species, with the latter presenting both cobalt monosilicide and dicobalt silicide. However, the catalytic activity of **AHCo2.5** was not as pronounced in terms of HGR as that of **PHCo2.5**, especially at the highest hydrolysis temperature tested.

Lale et al. (2017) previously demonstrated that composites containing carbon exhibit lower activity in the hydrolysis of $NaBH_4$, aligning with a preference for nitrides. Hence, one of the potential explanations for the performance of **PHCo2.5** is the presence of cobalt silicide species combined with the lower concentration of carbon atoms in this sample, which enhance the hydrolysis of $NaBH_4$ at high temperatures.

Table 6 shows a compilation with some selected data from the recent literature with cobalt-based catalysts, to comparison with the obtained results in the present work.

Table 6 – Test temperatures and HGR for different Co-based catalysts.

Material	**T (K)**	**HGR (mL min^{-1} $g_{cat}{}^{-1}$)**	**Reference**
Co/$Ti_4N_3T_x$	303 - 333	526	Tianshuo Li et al. (2021)
Co/CuO–NiO–Al_2O_3	298 - 328	6460	Erat et al. (2022)
Co/Fe_3O_4@C	288 - 328	1403	Bo Chen et al. (2018)
Fe_3O_4@C–Co	298	1746	Baye et al. (2019)
Co@PTA@Fe_3O_4@KLN	303	1540	Ecer et al. (2023)

Source: Author (2023).

In terms of HGR values, when comparing the ones obtained between 298 and 333 K, it is possible to observe that the materials produced here present lower values than those shown in Table 6. However, with the increase in temperature the cobalt-based PDC presented impressive HGR values, with 3,969.13 mL min^{-1} $g_{cat}{}^{-1}$ for **AHCo2.5**. Furthermore, as the effect of temperature is distinctly very important in the reaction, the test at four different temperatures proved essential to investigate this influence.

It is worth mentioning that the majority of cobalt-based materials are typically assessed in hydrolysis reactions within the temperature range up to 318 or 328 K, which

can pose challenges when trying to carry out a more comprehensive comparison at elevated temperatures. Also, as (UGALE et al., 2022; SUN et al., 2022).

There are many other factors that influence HGR besides temperature in the $NaBH_4$ hydrolysis reaction, that are $NaBH_4$ concentration, NaOH concentration, catalyst amount and metal ratio and distribution (SHU et al., 2019; LI, T. et al., 2021; ERAT et al., 2022). No statements can be made about the effect of each of these variables in this work because a kinetic study of the reaction was not carried out. Therefore, aiming to understand the kinetics parameters associated with the $NaBH_4$ hydrolysis reaction using the cobalt-doped PDC produced in the present work, more experiments are needed to evaluate the parameters mentioned above.

4.3.1 Reuse of catalysts

An extremely important characteristic that a catalyst must present is the possibility of reuse. This enables to reduce the overall cost of the process. In order to test reusability, the catalyst that presented the highest HGR value at a temperature of 353 K was chosen, that is, **PHCo2.5**. It was tested in hydrolysis following the same procedure previously described in the first use, and in subsequent uses, opening the reaction flask and only adding new loads of water, NaOH and $NaBH_4$, and maintaining the temperature at 353 K.

As expected, the materials proved to be very resistant to the conditions to which they were subjected, a result that was already expected for ceramics produced through the PDC route. The catalyst showed a reduction of only 26% in the conversion of $NaBH_4$ into H_2, after four consecutive cycles, demonstrating a great performance. This behaviour can be observed in 25(b). Also, a decrease in the HGR was also observed, as showed in Figure 25(a).

This is because it is carried out in a highly alkaline environment (pH > 12) and many catalytic supports do not withstand such conditions.

Figure 25 – Reuse of **PHCo2.5** in terms of (a) H_2 volume and (b) $NaBH_4$ conversion.

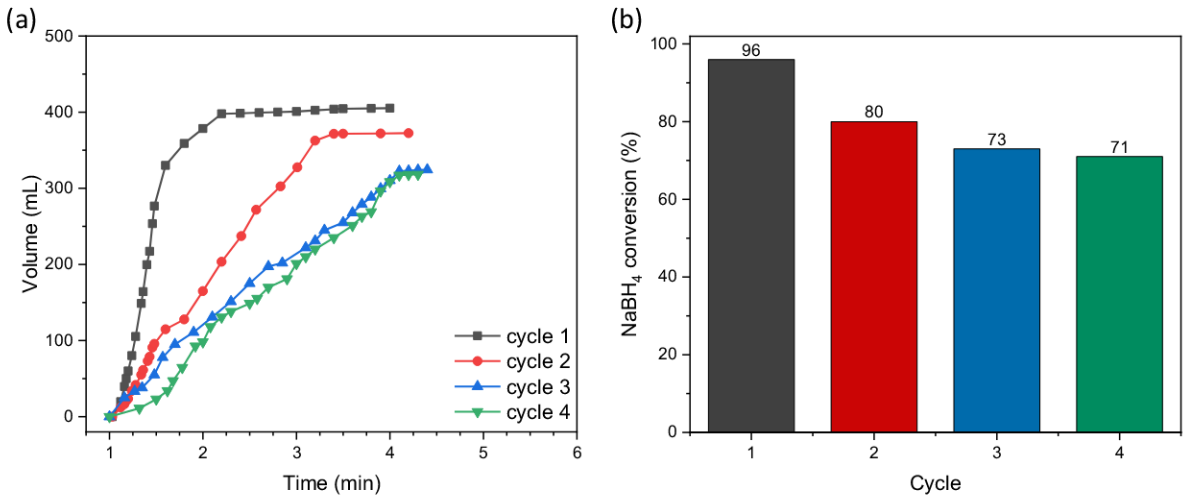

Source: Author (2023).

A very similar behaviour as observed here was already been reported in the literature for cobalt-based catalysts, with decrease in conversion of $NaBH_4$ into H_2 after only a few cycles, without washing (AKDIM et al., 2011; DEMIRCI, Umit B.; MIELE,

Philippe, 2014b; ECER et al., 2023). Many results found in the literature do not provide data in terms of $NaBH_4$ conversion, therefore this comparison cannot be made.

The deactivation of catalysts and consequent decrease in the $NaBH_4$ conversion, is attributed to the adsorption and/or deposition of borate species over the catalyst surface, and this phenomena is typical of cobalt-based catalysts. There is also the so-called "memory effect" when the catalyst is used during consecutive cycles, that is, without being removed from the solution medium, which is the case in the present work (AKDIM et al., 2011; DEMIRCI, Umit B.; MIELE, Philippe, 2014a; GAO et al., 2019; SIMAGINA et al., 2021; HANSU, 2023).

After being used consecutively for 4 cycles, the catalyst was subjected to the washing procedure, in order to test whether its conversion capacity would be regenerated. A comparison between the conversion before and after washing is showed in the Figure 26. It is possible to observe that the loss in conversion of around 29% for the washed catalyst, and also that conversion capacity was not recovered with this washing procedure.

Figure 26 – Comparison terms of $NaBH_4$ conversion in reuse of **PHCo2.5**, before and after washing with water.

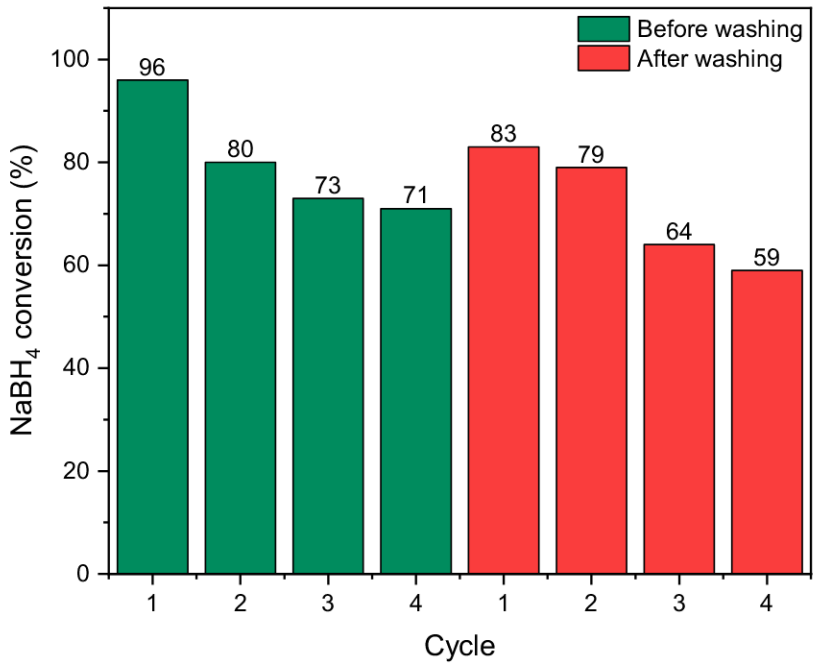

Source: Author (2023).

Clearly, the conversion capacity drastically decreased from the first use (96%) to the last (59%), even after washing. This indicates that catalyst deactivation was not reversed by using water washing. This was already reported in the literature for cobalt-containing catalysts. It is believed that borates interact strongly with cobalt particles through Co-O-B interactions and also in interactions with each other through B-O-B bridges. This makes it difficult to reactivate the catalyst, and it has been reported that washing with water alone is not sufficient to remove borates from the surface. (AKDIM et al., 2011; DEMIRCI, Umit B.; MIELE, Philippe, 2014a; GAO et al., 2019; SIMAGINA et al., 2021; HANSU, 2023).

The so-called "memory effect" is the *in-situ* formation of borates and/or polyborates ($B_\alpha O_\beta (OH)^{-}\gamma$) thick layer over the catalyst surface, proved by Umit B. Demirci

and Philippe Miele (2014a) and by Akdim et al. (2011) trough XPS and SEM analysis. This layer is not removed from the surface by using washing method with water, but with a dilute acid solution, and so partial reactivation of catalyst is achieved. Results indicate that the acid-washing can be done *in-situ*, by only adding the acid solution to the system, but studies using this approach are still in progress (DEMIRCI, Umit B.; MIELE, Philippe, 2014a; AKDIM et al., 2011; ARZAC, G. et al., 2012; GAO et al., 2019).

The results presented here showed that the **PHCo2.5** catalyst is very promising for use in hydrolysis reactions, therefore reinforcing the importance of further studies based on this material and its characteristics.

5 CONCLUSION

In this research work, three polymer-derived ceramic materials doped with cobalt were developed. Cobalt (II) chloride was used as metallic precursor and three different preceramic polymers: Allylhydridopolycarbosilane (AHPCS), Perhydropolysilazane (PHPS) and Poly(methylvinyl)silazane (HTT). The characterizations carried out on the material showed that silicon-based ceramics doped with cobalt were successfully obtained through the PDC route.

The methodology for synthesizing ceramics using the PDC route was proved, once again, to be extremely interesting as it is a single-step route, achieving the desired changes in the final ceramic produced. The heat treatment was carried out at low temperature of 1000 ℃, making the processing less energy-intensive compared to traditional ceramic processing, which uses higher temperatures.

The materials produced were tested as catalysts in the sodium borohydride hydrolysis reaction, aiming to generate hydrogen from this solid hydride that could enable the future use of the gas. Furthermore, such a reaction is extremely important in order to test the chemical resistance of the materials produced. The materials proved to be very resistant to the conditions to which they were subjected, a result that was already expected as ceramics produced through the PDC route are known to have high chemical resistance.

Furthermore, the materials showed different hydrogen generation at the four temperatures tested. Hydrogen generation rate values were obtained in the range of 34 to 7641 ml min^{-1} $g_{cat}{}^{-1}$, with the best result being 7142 ml min^{-1} $g_{cat}{}^{-1}$ for the catalyst **PHCo2.5** tested at 80 ℃ (353 K). Also, this catalyst was subjected to continuous reuse tests. Interesting results were obtained, where after four cycles of continuous reuse, the catalyst showed a 26% drop in the conversion of Na to H2. The catalyst was then washed with water successive times to remove borates (co-products of the hydrolysis reaction) and after drying it was tested again in the reaction. This time, after four cycles of use, the material showed a 29% drop in conversion, which shows that washing with water alone was not enough to reactivate the catalyst.

The obtained result shows that the materials produced have good potential to be explored to be used as catalytic supports for the $NaBH_4$ hydrolysis reaction. Catalytic supports produced via the PDC route are very promising materials and hopefully this work will contribute to the development of new technologies in the context of a future based on clean energy sources and renewable energy vectors such as hydrogen.

6 SUGGESTIONS FOR FUTURE RESEARCH

• For a better understanding of the role of cobalt-based PDC catalysts, it is suggested to carry out detailed kinetic studies, such as variation in reagent concentrations, pH of the reaction medium and variation in the amount of catalyst.

• The utilization of other characterization techniques is suggested to obtain more detailed information about the morphology and composition of cobalt-based PDC catalysts. Namely, FRX (to obtain composition information), SEM-EDX (to obtain morphological information and surface element distribution), TG-MS (to ensure the composition of mass losses during heat treatment), and crystallite size analysis to ascertain the formation of cobalt nanocrystals.

• Finally, the production and testing of bimetallic PDC catalysts (such as Cobalt-Nickel for example) can be very promising, since bimetallic catalysts are reported to have excellent catalytic response in the $NaBH_4$ hydrolysis reaction.

REFERENCES

ABDELHAMID, Hani Nasser. A review on hydrogen generation from the hydrolysis of sodium borohydride. **International Journal of Hydrogen Energy**, v. 46, 1 2021. ISSN 03603199. DOI: 10.1016/j.ijhydene.2020.09.186.

ACAR, Canan; DINCER, Ibrahim. The potential role of hydrogen as a sustainable transportation fuel to combat global warming. **International Journal of Hydrogen Energy**, v. 45, p. 3396–3406, 5 Jan. 2020. ISSN 03603199. DOI: 10.1016/j.ijhydene.2018.10.149.

ACHESON, Edward. Production of artifcial crystalline carbonaceous materials US Patent 492767, 1893.

ACKLEY, Brandon J. et al. Advances in the Synthesis of Preceramic Polymers for the Formation of Silicon-Based and Ultrahigh-Temperature Non-Oxide Ceramics. **Chemical Reviews**, v. 123, p. 4188–4236, 8 Apr. 2023. ISSN 0009-2665. DOI: 10.1021/acs.chemrev.2c00381.

ACOSTA, Emanoelle Diz. **Boron Modified Silicon Carbide By PDC Route: Dense and Porous Ceramics**. 2019. S. 225. PhD thesis – Universidade Federal de Santa Catarina, Florianópolis.

AINGER, FW; HERBERT, JM. The preparation of phosphorus-nitrogen compounds as non-porous solids. In: WILEY-V CH VERLAG GMBH MUHLENSTRASSE 33-34, D-13187 BERLIN, GERMANY, 20. ANGEWANDTE CHEMIE-INTERNATIONAL EDITION. [S.l.: s.n.], 1959. P. 653–653.

AJANOVIC, A.; SAYER, M.; HAAS, R. The economics and the environmental benignity of different colors of hydrogen. **International Journal of Hydrogen Energy**, v. 47, p. 24136–24154, 57 July 2022. ISSN 03603199. DOI: 10.1016/j.ijhydene.2022.02.094.

AL-AJRASH, Saja M. Nabat; BROWNING, Charles; ECKERLE, Rose; CAO, Li. Initial development of preceramic polymer formulations for additive manufacturing. **Materials Advances**, v. 2, p. 1083–1089, 3 2021. ISSN 2633-5409. DOI: 10.1039/D0MA00742K.

AKDIM, Ouardia; DEMIRCI, Umit B.; MIELE, Philippe. Deactivation and reactivation of cobalt in hydrolysis of sodium borohydride. **International Journal of Hydrogen Energy**, v. 36, p. 13669–13675, 21 Oct. 2011. ISSN 03603199. DOI: 10.1016/j.ijhydene.2011.07.125.

ANHUA, Liu; JIANMING, Chen; SHAONAN, Ding; YANBO, Yao; LING, Liu; FENGPING, Li; LIFU, Chen. Processing and characterization of cobalt silicide nanoparticle-containing silicon carbide fibers through a colloidal method and their

underlying mechanism. **J. Mater. Chem. C**, v. 2, p. 4980–4988, 25 2014. ISSN 2050-7526. DOI: 10.1039/C4TC00315B.

ARCOS, Jose M. Marín; SANTOS, Diogo M. F. The Hydrogen Color Spectrum: Techno-Economic Analysis of the Available Technologies for Hydrogen Production. **Gases**, v. 3, p. 25–46, 1 Feb. 2023. ISSN 2673-5628. DOI: 10.3390/gases3010002.

ARSAD, A.Z.; HANNAN, M.A.; AL-SHETWI, Ali Q.; MANSUR, M.; MUTTAQI, K.M.; DONG, Z.Y.; BLAABJERG, F. Hydrogen energy storage integrated hybrid renewable energy systems: A review analysis for future research directions. **International Journal of Hydrogen Energy**, v. 47, p. 17285–17312, 39 May 2022. ISSN 03603199. DOI: 10.1016/j.ijhydene.2022.03.208.

ARZAC, G. M.; FERNÁNDEZ, A. Advances in the implementation of PVD-based techniques for the preparation of metal catalysts for the hydrolysis of sodium borohydride. **International Journal of Hydrogen Energy**, v. 45, 58 2020. ISSN 03603199. DOI: 10.1016/j.ijhydene.2020.09.041.

ARZAC, G.M.; HUFSCHMIDT, D.; HARO, M.C. Jiménez De; FERNÁNDEZ, A.; SARMIENTO, B.; JIMÉNEZ, M.A.; JIMÉNEZ, M.M. Deactivation, reactivation and memory effect on Co–B catalyst for sodium borohydride hydrolysis operating in high conversion conditions. **International Journal of Hydrogen Energy**, v. 37, p. 14373–14381, 19 Oct. 2012. ISSN 03603199. DOI: 10.1016/j.ijhydene.2012.06.117.

ASAKUMA, Norifumi; TADA, Shotaro; KAWAGUCHI, Erika; TERASHIMA, Motoharu; HONDA, Sawao; NISHIHORA, Rafael Kenji; CARLES, Pierre; BERNARD, Samuel; IWAMOTO, Yuji. Mechanistic Investigation of the Formation of Nickel Nanocrystallites Embedded in Amorphous Silicon Nitride Nanocomposites. **Nanomaterials**, v. 12, p. 1644, 10 May 2022. ISSN 2079-4991. DOI: 10.3390/nano12101644.

AWIN, Eranezhuth Wasan; GÜNTHER, Timon E.; LOUKRAKPAM, Rameshwori; SCHAFFÖNER, Stefan; ROTH, Christina; MOTZ, Günter. Synthesis and characterization of precursor derived TiN@Si–Al–C–N ceramic nanocomposites for oxygen reduction reaction. **International Journal of Applied Ceramic Technology**, v. 20, p. 59–69, 1 Jan. 2023. ISSN 1546-542X. DOI: 10.1111/ijac.14234.

BARROSO, Gilvan; LI, Quan; BORDIA, Rajendra K.; MOTZ, Günter. Polymeric and ceramic silicon-based coatings – a review. **Journal of Materials Chemistry A**, v. 7, p. 1936–1963, 5 2019. ISSN 2050-7488. DOI: 10.1039/C8TA09054H.

BARROSO, Gilvan S.; KRENKEL, Walter; MOTZ, Günter. Low thermal conductivity coating system for application up to 1000 ℃ by simple PDC processing with active and passive fillers. **Journal of the European Ceramic Society**, v. 35, p. 3339–3348, 12 Oct. 2015. ISSN 09552219. DOI: 10.1016/j.jeurceramsoc.2015.02.006.

BARTLETT, Jay; KRUPNICK, Alan. **Resources For the Future — Investment Tax Credits for Hydrogen Storage**. [S.l.: s.n.], 2020. https://www.rff.org/publications/issue-briefs/investment-tax-credits-hydrogen-storage/.

BAYE, Anteneh F.; ABEBE, Medhen W.; APPIAH-NTIAMOAH, Richard; KIM, Hern. Engineered iron-carbon-cobalt (Fe3O4@C-Co) core-shell composite with synergistic catalytic properties towards hydrogen generation via NaBH4 hydrolysis. **Journal of Colloid and Interface Science**, v. 543, p. 273–284, May 2019. ISSN 00219797. DOI: 10.1016/j.jcis.2019.02.065.

BERNARD, Samuel; MIELE, Philippe. Polymer-derived boron nitride: A review on the chemistry, shaping and ceramic conversion of borazine derivatives. **Materials**, v. 7, 11 2014. ISSN 19961944. DOI: 10.3390/ma7117436.

CHAUDHARY, Raghvendra Pratap; PARAMESWARAN, Chithra; IDREES, Muhammad; RASAKI, Abolaji Sefiu; LIU, Changyong; CHEN, Zhangwei; COLOMBO, Paolo. Additive manufacturing of polymer-derived ceramics: Materials, technologies, properties and potential applications. **Progress in Materials Science**, v. 128, p. 100969, July 2022. ISSN 00796425. DOI: 10.1016/j.pmatsci.2022.100969.

CHEN, Bo; CHEN, Sijiang; BANDAL, Harshad A.; APPIAH-NTIAMOAH, Richard; JADHAV, Amol R.; KIM, Hern. Cobalt nanoparticles supported on magnetic core-shell structured carbon as a highly efficient catalyst for hydrogen generation from NaBH 4 hydrolysis. **International Journal of Hydrogen Energy**, v. 43, p. 9296–9306, 19 May 2018. ISSN 03603199. DOI: 10.1016/j.ijhydene.2018.03.193.

CHEN, Qi; ZHANG, Xiaosong; WANG, Feng. Experimental study of thermal diffusion enhanced vapor transfer performance with perhydropolysilazane-derived silica (PDS) coating membranes in air dehumidification process. **International Journal of Refrigeration**, v. 122, p. 21–32, Feb. 2021. ISSN 01407007. DOI: 10.1016/j.ijrefrig.2020.11.003.

CHEN, Xiao; LIANG, Changhai. Transition metal silicides: fundamentals, preparation and catalytic applications. **Catalysis Science Technology**, v. 9, p. 4785–4820, 18 2019. ISSN 2044-4753. DOI: 10.1039/C9CY00533A.

COLOMBO, Paolo; MERA, Gabriela; BROWN, H. C; GILBREATH, J. R. Polymer-derived ceramics:40 years of research and innovation in advanced ceramics. **Journal of the American Ceramic Society**, v. 97, n. 1, p. 1805–1837, 2010.

DAWOOD, Furat; ANDA, Martin; SHAFIULLAH, G.M. Hydrogen production for energy: An overview. **International Journal of Hydrogen Energy**, v. 45, p. 3847–3869, 7 Feb. 2020. ISSN 03603199. DOI: 10.1016/j.ijhydene.2019.12.059.

DEMIRCI, U. B.; MIELE, P. Cobalt in NaBH4 hydrolysis. **Physical Chemistry Chemical Physics**, v. 12, p. 14651, 44 2010. ISSN 1463-9076. DOI: 10.1039/c0cp00295j.

DEMIRCI, Umit B.; MIELE, Philippe. Cobalt-based catalysts for the hydrolysis of NaBH4 and NH3BH3. **Physical Chemistry Chemical Physics**, v. 16, p. 6872, 15 2014a. ISSN 1463-9076. DOI: 10.1039/c4cp00250d.

DEMIRCI, Umit B.; MIELE, Philippe. Reaction mechanisms of the hydrolysis of sodium borohydride: A discussion focusing on cobalt-based catalysts. **Comptes Rendus Chimie**, v. 17, p. 707–716, 7-8 July 2014b. ISSN 16310748. DOI: 10.1016/j.crci.2014.01.012.

DOE. **Hydrogen Storage - Hydrogen and Fuel Cell Technologies Office**. [S.l.: s.n.], 2023. https://www.energy.gov/eere/fuelcells/hydrogen-storage.

DUO, Leijiao; ZHANG, Zongbo; ZHENG, Kun; WANG, Dan; XU, Caihong; XIA, Yuzheng. Perhydropolysilazane derived SiON interfacial layer for Cu/epoxy molding compound composite. **Surface and Coatings Technology**, v. 391, p. 125703, June 2020. ISSN 02578972. DOI: 10.1016/j.surfcoat.2020.125703.

ECER, Ümit; ZENGIN, Adem; ŞAHAN, Tekin. Fabrication and characterization of poly(tannic acid) coated magnetic clay decorated with cobalt nanoparticles for NaBH4 hydrolysis: RSM-CCD based modeling and optimization. **International Journal of Hydrogen Energy**, v. 48, p. 23620–23632, 61 July 2023. ISSN 03603199. DOI: 10.1016/j.ijhydene.2023.03.125.

ERAT, Neslihan; BOZKURT, Gamze; ÖZER, Abdulkadir. Co/CuO–NiO–Al2O3 catalyst for hydrogen generation from hydrolysis of NaBH4. **International Journal of Hydrogen Energy**, v. 47, p. 24255–24267, 58 July 2022. ISSN 03603199. DOI: 10.1016/j.ijhydene.2022.05.178.

FENG, Yao. **Single-source-precursor synthesized SiC-based nanocomposites with an in-situ formed Nowotny phase as multifunctional materials for electrocatalytic and electromagnetic wave absorbing applications**. 2020. S. 121. PhD thesis – Technische Universität Darmstadt, Darmstadt.

FERREIRA, Roberta Karoline Morais et al. Low temperature in situ immobilization of nanoscale fcc and hcp polymorphic nickel particles in polymer-derived Si–C–O–N(H) to promote electrocatalytic water oxidation in alkaline media. **Nanoscale Advances**, v. 5, p. 701–710, 3 2023. ISSN 2516-0230. DOI: 10.1039/D2NA00821A.

FLORES, Octavio; SCHMALZ, Thomas; KRENKEL, Walter; HEYMANN, Lutz; MOTZ, Günter. Selective cross-linking of oligosilazanes to tailored meltable polysilazanes for the processing of ceramic SiCN fibres. **Journal of Materials Chemistry A**, v. 1, p. 15406, 48 2013. ISSN 2050-7488. DOI: 10.1039/c3ta13254d.

FU, Shengyang; ZHU, Min; ZHU, Yufang. Organosilicon polymer-derived ceramics: An overview. **Journal of Advanced Ceramics**, v. 8, p. 457–478, 4 Dec. 2019. ISSN 2226-4108. DOI: 10.1007/s40145-019-0335-3.

GAO, Zhiting; DING, Chuanmin; WANG, Junwen; DING, Guangyue; XUE, Yanan; ZHANG, Yongkang; ZHANG, Kan; LIU, Ping; GAO, Xiaofeng. Cobalt nanoparticles packaged into nitrogen-doped porous carbon derived from metal-organic framework nanocrystals for hydrogen production by hydrolysis of sodium borohydride. **International Journal of Hydrogen Energy**, v. 44, p. 8365–8375, 16 Mar. 2019. ISSN 03603199. DOI: 10.1016/j.ijhydene.2019.02.008.

HANNIET, Quentin. **Design of new Polymer-Derived Ceramic based electrodes for Hydrogen Evolution Reaction**. 2021. PhD thesis – École Nationale Supérieure de Chimie Montpellier, Montpellier.

HANSU, Tülin Avcı. A novel and active ruthenium based supported multiwalled carbon nanotube tungsten nanoalloy catalyst for sodium borohydride hydrolysis. **International Journal of Hydrogen Energy**, v. 48, p. 6788–6797, 18 Feb. 2023. ISSN 03603199. DOI: 10.1016/j.ijhydene.2022.04.269.

HERMESMANN, M.; MÜLLER, T.E. Green, Turquoise, Blue, or Grey? Environmentally friendly Hydrogen Production in Transforming Energy Systems. **Progress in Energy and Combustion Science**, v. 90, p. 100996, May 2022. ISSN 03601285. DOI: 10.1016/j.pecs.2022.100996.

HUA, D; HANXI, Y; XINPING, A; CHUANSIN, C. Hydrogen production from catalytic hydrolysis of sodium borohydride solution using nickel boride catalyst. **International Journal of Hydrogen Energy**, v. 28, p. 1095–1100, 10 Oct. 2003. ISSN 03603199. DOI: 10.1016/S0360-3199(02)00235-5.

IEA. **International Energy Agency - Hydrogen Projects Database**. [S.l.: s.n.], 2023. https://www.iea.org/data-and-statistics/data-product/hydrogen-projects-database.

INCER-VALVERDE, Jimena; KORAYEM, Amira; TSATSARONIS, George; MOROSUK, Tatiana. “Colors” of hydrogen: Definitions and carbon intensity. **Energy Conversion and Management**, v. 291, p. 117294, Sept. 2023. ISSN 01968904. DOI: 10.1016/j.enconman.2023.117294.

IONESCU, Emanuel; KLEEBE, Hans-Joachim; RIEDEL, Ralf. Silicon-containing polymer-derived ceramic nanocomposites (PDC-NCs): preparative approaches and properties. **Chemical Society Reviews**, v. 41, p. 5032, 15 2012. ISSN 0306-0012. DOI: 10.1039/c2cs15319j.

IPCC. IPCC, 2023: Summary for Policymakers. In: Climate Change 2023: Synthesis Report. A Report of the Intergovernmental Panel on Climate Change. IPCC, Geneva, Switzerland, 36 pages. (in press)., 2023.

ISHAQ, Haris; DINCER, Ibrahim; CRAWFORD, Curran. A review on hydrogen production and utilization: Challenges and opportunities. **International Journal of Hydrogen Energy**, v. 47, p. 26238–26264, 62 July 2022. ISSN 03603199. DOI: 10.1016/j.ijhydene.2021.11.149.

KAUR, Arshdeep; GANGACHARYULU, Dasaroju; BAJPAI, Pramod K. KINETIC STUDIES OF HYDROLYSIS REACTION OF NaBH4 WITH Al2O3 NANOPARTICLES AS CATALYST PROMOTER AND CoCl2 AS CATALYST. **Brazilian Journal of Chemical Engineering**, v. 36, p. 929–939, 2 June 2019. ISSN 1678-4383. DOI: 10.1590/0104-6632.20190362s20180290.

KAUR, Sarabjeet. **Single-Source-Precursor Synthesis of SiC-Based Ceramic Nanocomposites for EnergyRelated Applications**. 2016. S. 191. PhD thesis – Technische Universität Darmstadt, Darmstadt.

KAUR, Sarabjeet; RIEDEL, Ralf; IONESCU, Emanuel. Pressureless fabrication of dense monolithic SiC ceramics from a polycarbosilane. **Journal of the European Ceramic Society**, v. 34, p. 3571–3578, 15 Dec. 2014. ISSN 09552219. DOI: 10.1016/j.jeurceramsoc.2014.05.002.

KIM, JooHyung; YANG, JungYup; LEE, JunSeok; HONG, JinPyo. Memory characteristics of cobalt-silicide nanocrystals embedded in HfO2 gate oxide for nonvolatile nanocrystal flash devices. **Applied Physics Letters**, v. 92, 1 Jan. 2008. ISSN 0003-6951. DOI: 10.1063/1.2831667.

KOJIMA, Yoshitsugu. Hydrogen storage materials for hydrogen and energy carriers. **International Journal of Hydrogen Energy**, v. 44, p. 18179–18192, 33 2019. ISSN 03603199. DOI: 10.1016/j.ijhydene.2019.05.119.

KUMAR, S. Shiva; LIM, Hankwon. An overview of water electrolysis technologies for green hydrogen production. **Energy Reports**, v. 8, p. 13793–13813, Nov. 2022. ISSN 23524847. DOI: 10.1016/j.egyr.2022.10.127.

KYTSYA, A.; BEREZOVETS, V.; VERBOVYTSKYY, Yu.; BAZYLYAK, L.; KORDAN, V.; ZAVALIY, I.; YARTYS, V.A. Bimetallic Ni-Co nanoparticles as an efficient catalyst of hydrogen generation via hydrolysis of NaBH4. **Journal of Alloys and Compounds**, v. 908, p. 164484, July 2022. ISSN 09258388. DOI: 10.1016/j.jallcom.2022.164484.

LALE, Abhijeet; PROUST, Vanessa; BECHELANY, Mirna Chaker; VIARD, Antoine; MALO, Sylvie; BERNARD, Samuel. A comprehensive study on the influence of the polyorganosilazane chemistry and material shape on the high temperature behavior of titanium nitride/silicon nitride nanocomposites. **Journal of the European Ceramic Society**, v. 37, p. 5167–5175, 16 Dec. 2017. ISSN 09552219. DOI: 10.1016/j.jeurceramsoc.2017.04.001.

LALE, Abhijeet; SCHMIDT, Marion; MALLMANN, Maíra Debarba; BEZERRA, André Vinícius Andrade; ACOSTA, Emanoelle Diz; MACHADO, Ricardo Antonio Francisco; DEMIRCI, Umit B.; BERNARD, Samuel. Polymer-Derived Ceramics with engineered mesoporosity: From design to application in catalysis. **Surface and Coatings Technology**, v. 350, p. 569–586, Sept. 2018. ISSN 02578972. DOI: 10.1016/j.surfcoat.2018.07.061.

LALE, Abhijeet; WASAN, Awin; KUMAR, Ravi; MIELE, Philippe; DEMIRCI, Umit B.; BERNARD, Samuel. Organosilicon polymer-derived mesoporous 3D silicon carbide, carbonitride and nitride structures as platinum supports for hydrogen generation by hydrolysis of sodium borohydride. **International Journal of Hydrogen Energy**, v. 41, p. 15477–15488, 34 Sept. 2016. ISSN 03603199. DOI: 10.1016/j.ijhydene.2016.06.186.

LALE, Abhijeet et al. Highly active, robust and reusable micro-/mesoporous TiN/Si3N4 nanocomposite-based catalysts for clean energy: Understanding the key role of TiN nanoclusters and amorphous Si3N4 matrix in the performance of the catalyst system. **Applied Catalysis B: Environmental**, Elsevier, v. 272, p. 118975, 2020. ISSN 0926-3373. DOI: 10.1016/J.APCATB.2020.118975.

LI, Ran; ZHANG, Fengming; ZHANG, Jiapeng; DONG, Hua. Catalytic hydrolysis of NaBH4 over titanate nanotube supported Co for hydrogen production. **International Journal of Hydrogen Energy**, v. 47, p. 5260–5268, 8 Jan. 2022. ISSN 03603199. DOI: 10.1016/j.ijhydene.2021.11.143.

LI, Tianshuo; XIANG, Cuili; ZOU, Yongjin; XU, Fen; SUN, Lixian. Synthesis of highly stable cobalt nanorods anchored on a Ti4N3Tx MXene composite for the hydrolysis of sodium borohydride. **Journal of Alloys and Compounds**, Elsevier, v. 885, p. 160991, 2021.

LI, Yuxin et al. Photo-thermal synergic enhancement of Co FeAl-LDHs for hydrogen generation from hydrolysis of NaBH4. **Applied Surface Science**, v. 610, p. 155325, Feb. 2023. ISSN 01694332. DOI: 10.1016/j.apsusc.2022.155325.

LUO, Rong; LI, Ruixiang; JIANG, Chunli; QI, Ruijuan; LIU, Mengqin; LUO, Chunhua; LIN, Hechun; HUANG, Rong; PENG, Hui. Facile synthesis of cobalt modified 2D titanium carbide with enhanced hydrogen evolution performance in alkaline media. **International Journal of Hydrogen Energy**, v. 46, p. 32536–32545, 64 Sept. 2021. ISSN 03603199. DOI: 10.1016/j.ijhydene.2021.07.110.

MAKIABADI, Mosadegheh; SHAMSPUR, Tayebeh; MOSTAFAVI, Ali. Performance improvement of oxygen on the carbon substrate surface for dispersion of cobalt nanoparticles and its effect on hydrogen generation rate via NaBH4 hydrolysis. **International Journal of Hydrogen Energy**, v. 45, p. 1706–1718, 3 Jan. 2020. ISSN 03603199. DOI: 10.1016/j.ijhydene.2019.11.026.

MALLMANN, Maíra et al. From polysilazanes to highly micro-/mesoporous Si3N4 containing in situ immobilized Co or Ni-based nanoparticles. **Polymer**, p. 126215, July 2023. ISSN 00323861. DOI: 10.1016/j.polymer.2023.126215.

MALLMANN, Maíra Debarba. **Polymer-derived mesoporous Si-M-N nanocomposites as co-catalysts for hydrogen evolution reactions**. 2020. S. 158. PhD thesis – Universidade Federal de Santa Catarina, Florianópolis.

MANJUNATHA, M.; REDDY, G. Srinivas; MALLIKARJUNAIAH, K. J.; DAMLE, Ramakrishna; RAMESH, K. P. Determination of Phase Composition of Cobalt Nanoparticles Using 59Co Internal Field Nuclear Magnetic Resonance. **Journal of Superconductivity and Novel Magnetism**, v. 32, p. 3201–3209, 10 Oct. 2019. ISSN 1557-1939. DOI: 10.1007/s10948-019-5083-7.

MAROCCO, Paolo; FERRERO, Domenico; LANZINI, Andrea; SANTARELLI, Massimo. The role of hydrogen in the optimal design of off-grid hybrid renewable energy systems. **Journal of Energy Storage**, v. 46, p. 103893, Feb. 2022. ISSN 2352152X. DOI: 10.1016/j.est.2021.103893.

MERA, Gabriela; GALLEI, Markus; BERNARD, Samuel; IONESCU, Emanuel. Ceramic Nanocomposites from Tailor-Made Preceramic Polymers. **Nanomaterials**, v. 5, p. 468–540, 2 Apr. 2015. ISSN 2079-4991. DOI: 10.3390/nano5020468.

MORADI, Ramin; GROTH, Katrina M. Hydrogen storage and delivery: Review of the state of the art technologies and risk and reliability analysis. **International Journal of Hydrogen Energy**, v. 44, p. 12254–12269, 23 May 2019. ISSN 03603199. DOI: 10.1016/j.ijhydene.2019.03.041.

NNABUIFE, Somtochukwu Godfrey; UGBEH-JOHNSON, Judith; OKEKE, Nonso Evaristus; OGBONNAYA, Chukwuma. Present and Projected Developments in Hydrogen Production: A Technological Review*. **Carbon Capture Science and Technology**, v. 3, p. 100042, June 2022. ISSN 27726568. DOI: 10.1016/j.ccst.2022.100042.

OSMAN, Ahmed I.; MEHTA, Neha; ELGARAHY, Ahmed M.; HEFNY, Mahmoud; AL-HINAI, Amer; AL-MUHTASEB, Ala'a H.; ROONEY, David W. Hydrogen production, storage, utilisation and environmental impacts: a review. **Environmental Chemistry Letters**, v. 20, p. 153–188, 1 Feb. 2022. ISSN 1610-3653. DOI: 10.1007/s10311-021-01322-8.

PANCHENKO, V.A.; DAUS, Yu.V.; KOVALEV, A.A.; YUDAEV, I.V.; LITTI, Yu.V. Prospects for the production of green hydrogen: Review of countries with high potential. **International Journal of Hydrogen Energy**, v. 48, p. 4551–4571, 12 Feb. 2023. ISSN 03603199. DOI: 10.1016/j.ijhydene.2022.10.084.

PINTO, A; FALCAO, D; SILVA, R; RANGEL, C. Hydrogen generation and storage from hydrolysis of sodium borohydride in batch reactors. **International Journal of Hydrogen Energy**, v. 31, p. 1341–1347, 10 Aug. 2006. ISSN 03603199. DOI: 10.1016/j.ijhydene.2005.11.015.

PRINT, Lewis J.; LIGGAT, John J.; MOUG, Stan; SEATON, Helen; APPERLEY, David C. A Study of the Ceramicisation of Allylhydridopolycarbosilane by Thermal Volatilisation Analysis and Solid-State Nuclear Magnetic Resonance. **Silicon**, v. 15, p. 1355–1379, 3 Feb. 2023. ISSN 1876-990X. DOI: 10.1007/s12633-022-02072-0.

RAHMAN, Arif; SINGH, Ashish; HARIMKAR, Sandip P.; SINGH, Raman P. Mechanical characterization of fine grained silicon carbide consolidated using polymer pyrolysis and spark plasma sintering. **Ceramics International**, v. 40, p. 12081–12091, 8 Sept. 2014. ISSN 02728842. DOI: 10.1016/j.ceramint.2014.04.048.

RETNAMMA, Rajasree; YU, Lin; RANGEL, CMc; NOVAIS, Augusto Q; JOHNSON, Karl; MATHEWS, Michael A. Kinetics of self-hydrolysis of concentrated sodium borohydride solutions at high temperatures. In: AMERICAN Institute of Chemical Engineering (AIChE 2011) Annual Meeting. [S.l.: s.n.], 2011.

SCHLESINGER, H. I.; BROWN, H. C.; FINHOLT, A. E.; GILBREATH, J. R.; HOEKSTRA, H. R.; HYDE, E. K. Sodium Borohydride, Its Hydrolysis and its Use as a Reducing Agent and in the Generation of Hydrogen. **Journal of the American Chemical Society**, v. 75, n. 1, p. 215–219, 1953.

SCHMIDT, Marion et al. Molecular-Level Processing of Si-(B)-C Materials with Tailored Nano/Microstructures. **Chemistry - A European Journal**, v. 23, 67 2017. ISSN 15213765. DOI: 10.1002/chem.201703674.

SHU, Hongfei; LU, Lilin; ZHU, Shufang; LIU, Miaomiao; ZHU, Yin; NI, Jiaqi; RUAN, Zhuhua; LIU, Yi. Ultra small cobalt nanoparticles supported on MCM41: One-pot synthesis and catalytic hydrogen production from alkaline borohydride. **Catalysis Communications**, v. 118, p. 30–34, Jan. 2019. ISSN 15667367. DOI: 10.1016/j.catcom.2018.09.012.

SIMAGINA, Valentina I.; OZEROVA, Anna M.; KOMOVA, Oksana V.; NETSKINA, Olga V. Recent Advances in Applications of Co-B Catalysts in NaBH4-Based Portable Hydrogen Generators. **Catalysts**, v. 11, p. 268, 2 Feb. 2021. ISSN 2073-4344. DOI: 10.3390/catal11020268.

SMOKOVYCH, Iryna; KRÜGER, Manja; SCHEFFLER, Michael. Polymer derived ceramic materials from Si, B and MoSiB filler-loaded perhydropolysilazane precursor for oxidation protection. **Journal of the European Ceramic Society**, v. 39, p. 3634–3642, 13 Oct. 2019. ISSN 09552219. DOI: 10.1016/j.jeurceramsoc.2019.05.022.

SMYRNIOTI, Maria; IOANNIDES, Theophilos. Synthesis of Cobalt-Based Nanomaterials from Organic Precursors. In: [s.l.]: InTech, Dec. 2017. DOI: 10.5772/intechopen.70947.

SONG, Jinlin; LI, Ran; DONG, Hua. Controllable hydrogen production from NaBH4 hydrolysis promoted by acetic acid. **International Journal of Hydrogen Energy**, v. 48, p. 8093–8100, 22 Mar. 2023. ISSN 03603199. DOI: 10.1016/j.ijhydene.2022.11.204.

STANWELL. **True colours: What do the different colours of hydrogen mean?** [S.l.: s.n.], 2023. https://whatswatt.com.au/true-colours-what-do-the-different-colours-of-hydrogen-mean/.

SUN, Lei et al. Novel high dispersion and high stability cobalt-inlaid carbon sphere catalyst for hydrogen generation from the hydrolysis of sodium borohydride. **Fuel**, v. 310, p. 122276, Feb. 2022. ISSN 00162361. DOI: 10.1016/j.fuel.2021.122276.

TADA, Shotaro et al. Low temperature in situ formation of cobalt in silicon nitride toward functional nitride nanocomposites. **Chemical Communications**, v. 57, p. 2057–2060, 16 2021. ISSN 1359-7345. DOI: 10.1039/D0CC07366K.

TARHAN, Cevahir; ÇIL, Mehmet Ali. A study on hydrogen, the clean energy of the future: Hydrogen storage methods. **Journal of Energy Storage**, v. 40, p. 102676, Aug. 2021. ISSN 2352152X. DOI: 10.1016/j.est.2021.102676.

UGALE, Ashok D.; GHODKE, Neha P.; KANG, Gil-Seon; NAM, Ki-Bong; BHORASKAR, Sudha V.; MATHE, Vikas L.; YOO, Ji Beom. Cost-effective synthesis of carbon loaded Co3O4 for controlled hydrogen generation via NaBH4 hydrolysis. **International Journal of Hydrogen Energy**, v. 47, p. 16–29, 1 Jan. 2022. ISSN 03603199. DOI: 10.1016/j.ijhydene.2021.09.262.

VERBEEK, W; WINTER, G. Formkoerper aus Siliciumcarbid und Verfahren zu ihrer Herstellung Patent DE2236078, 1974.

WANG, Jun; GRÜNBACHER, Matthias; PENNER, Simon; BEKHEET, Maged F.; GURLO, Aleksander. Porous Silicon Oxycarbonitride Ceramics with Palladium and Pd2Si Nanoparticles for Dry Reforming of Methane. **Polymers**, v. 14, p. 3470, 17 Aug. 2022a. ISSN 2073-4360. DOI: 10.3390/polym14173470.

WANG, Jun; KOBER, Delf; SHAO, Gaofeng; EPPING, Jan Dirk; GÖRKE, Oliver; LI, Shuang; GURLO, Aleksander; BEKHEET, Maged F. Stable anodes for lithium-ion batteries based on tin-containing silicon oxycarbonitride ceramic nanocomposites. **Materials Today Energy**, v. 26, p. 100989, June 2022b. ISSN 24686069. DOI: 10.1016/j.mtener.2022.100989.

WANG, Jun; SCHÖLCH, Valérie; GÖRKE, Oliver; SCHUCK, Götz; WANG, Xifan; SHAO, Gaofeng; SCHORR, Susan; BEKHEET, Maged F.; GURLO, Aleksander. Metal-containing ceramic nanocomposites synthesized from metal acetates and polysilazane. **Open Ceramics**, v. 1, p. 100001, May 2020a. ISSN 26665395. DOI: 10.1016/j.oceram.2020.100001.

WANG, Jun; SCHÖLCH, Valérie; GÖRKE, Oliver; SCHUCK, Götz; WANG, Xifan; SHAO, Gaofeng; SCHORR, Susan; BEKHEET, Maged F.; GURLO, Aleksander. Metal-containing ceramic nanocomposites synthesized from metal acetates and polysilazane. **Open Ceramics**, v. 1, p. 100001, May 2020b. ISSN 26665395. DOI: 10.1016/j.oceram.2020.100001.

WANG, Qing; YOKOJI, Makoto; NAGASAWA, Hiroki; YU, Liang; KANEZASHI, Masakoto; TSURU, Toshinori. Microstructure evolution and enhanced permeation of SiC membranes derived from allylhydridopolycarbosilane. **Journal of Membrane Science**, v. 612, p. 118392, Oct. 2020. ISSN 03767388. DOI: 10.1016/j.memsci.2020.118392.

WANG, Wen-Yue; ZHANG, Yu-Lin; GUO, Xiang; WANG, Li-Ming; ZHANG, Jun-Rong; YANG, Hui; DONG, Guo-Jun; ZHANG, Zong-Bo; XU, Cai-Hong. Rapid Conversion of Perhydropolysilazane into Thin Silica Coating at Low Temperature. **Chinese Journal of Polymer Science**, Mar. 2023. ISSN 0256-7679. DOI: 10.1007/s10118-023-2959-6.

WEN, Qingbo; QU, Fangmu; YU, Zhaoju; GRACZYK-ZAJAC, Magdalena; XIONG, Xiang; RIEDEL, Ralf. Si-based polymer-derived ceramics for energy conversion and storage. **Journal of Advanced Ceramics**, v. 11, p. 197–246, 2 Feb. 2022. ISSN 2226-4108. DOI: 10.1007/s40145-021-0562-2.

WEN, Qingbo; YU, Zhaoju; RIEDEL, Ralf. The fate and role of in situ formed carbon in polymer-derived ceramics. **Progress in Materials Science**, v. 109, p. 100623, Apr. 2020. ISSN 00796425. DOI: 10.1016/j.pmatsci.2019.100623.

WINTER, Gerhard; VERBEEK, Wolfgang; MANSMANN, Manfred. Production of shaped articles of silicon carbide and silicon nitride, 1975.

XIE, Junfeng; XIE, Yi. Transition Metal Nitrides for Electrocatalytic Energy Conversion: Opportunities and Challenges. **Chemistry - A European Journal**, v. 22, p. 3588–3598, 11 2016. ISSN 09476539. DOI: 10.1002/chem.201501120.

YAJIMA, S.; HASEGAWA, Y.; OKAMURA, K.; MATSUZAWA, T. Development of high tensile strength silicon carbide fibre using an organosilicon polymer precursor. **Nature**, v. 273, p. 525–527, 5663 June 1978. ISSN 0028-0836. DOI: 10.1038/273525a0.

YANG, Le; ZHANG, Pei; FENG, Yao; YU, Zhaoju. Single-source-precursor synthesis and characterization of SiAlC(O) ceramics from a hyperbranched

polyaluminocarbosilane. **High Temperature Materials and Processes**, v. 41, p. 150–160, 1 Apr. 2022. ISSN 2191-0324. DOI: 10.1515/htmp-2022-0025.

ZAHEER, Muhammad; MOTZ, Günter; KEMPE, Rhett. The generation of palladium silicide nanoalloy particles in a SiCN matrix and their catalytic applications. **Journal of Materials Chemistry**, v. 21, p. 18825, 46 2011. FTIR - HTT. ISSN 0959-9428. DOI: 10.1039/c1jm13665h.

ZHAN, Ying et al. Boron-modified perhydropolysilazane towards facile synthesis of amorphous SiBN ceramic with excellent thermal stability. **Journal of Advanced Ceramics**, v. 11, p. 1104–1116, 7 July 2022. ISSN 2226-4108. DOI: 10.1007/s40145-022-0597-z.

ZHANG, Liangliang; CHEN, Xiao; CHEN, Yujing; PENG, Zhijian; LIANG, Changhai. Acid-tolerant intermetallic cobalt–nickel silicides as noble metal-like catalysts for selective hydrogenation of phthalic anhydride to phthalide. **Catalysis Science Technology**, v. 9, p. 1108–1116, 5 2019. ISSN 2044-4753. DOI: 10.1039/C8CY02258E.

ZHANG, Liangliang; CHEN, Xiao; JIN, Shaohua; GUAN, Jingchao; WILLIAMS, Christopher T.; PENG, Zhijian; LIANG, Changhai. Rapid microwaves synthesis of CoSix/CNTs as novel catalytic materials for hydrogenation of phthalic anhydride. **Journal of Solid State Chemistry**, v. 217, p. 105–112, Sept. 2014. ISSN 00224596. DOI: 10.1016/j.jssc.2014.05.021.

ZHANG, Liangliang; CHEN, Xiao; LI, Chuang; ARMBRÜSTER, Marc; PENG, Zhijian; LIANG, Changhai. Cobalt Silicides Nanoparticles Embedded in N-Doped Carbon as Highly Efficient Catalyst in Selective Hydrogenation of Cinnamaldehyde. **ChemistrySelect**, v. 3, p. 1658–1666, 6 Feb. 2018. ISSN 23656549. DOI: 10.1002/slct.201800007.

APPENDIX A – XPS SURVEY SPECTRA

Figure 27 – Survey spectrum for AHCo2.5.

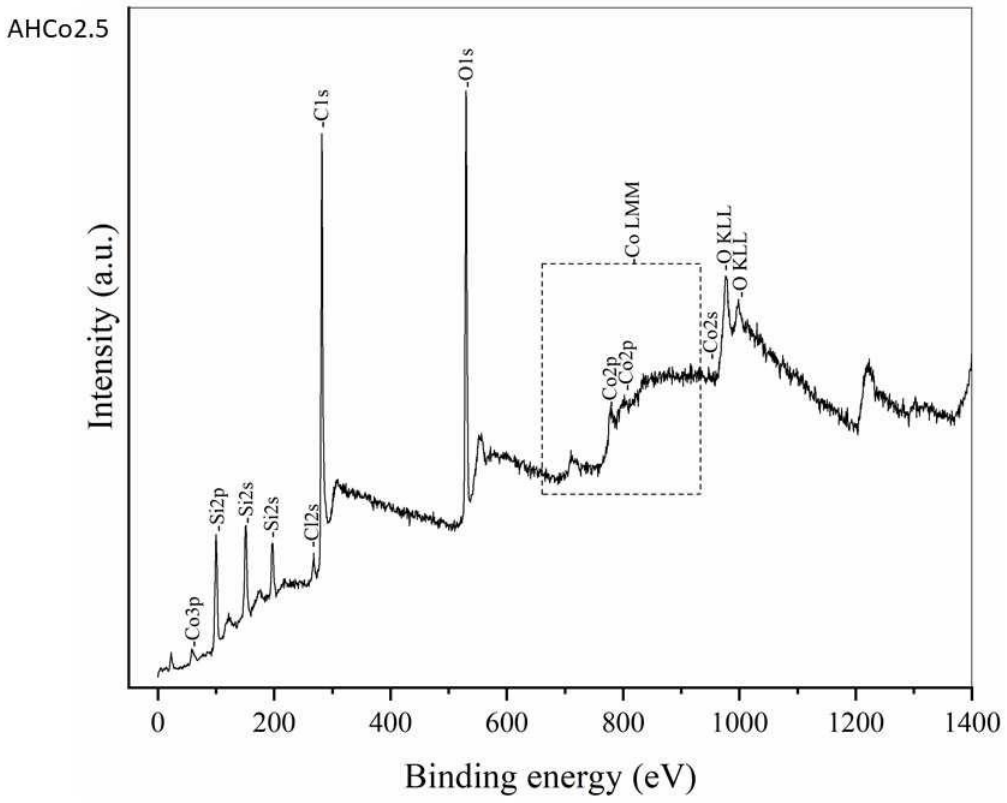

Source: Author (2023).

Figure 28 – Survey spectrum for HTCo2.5.

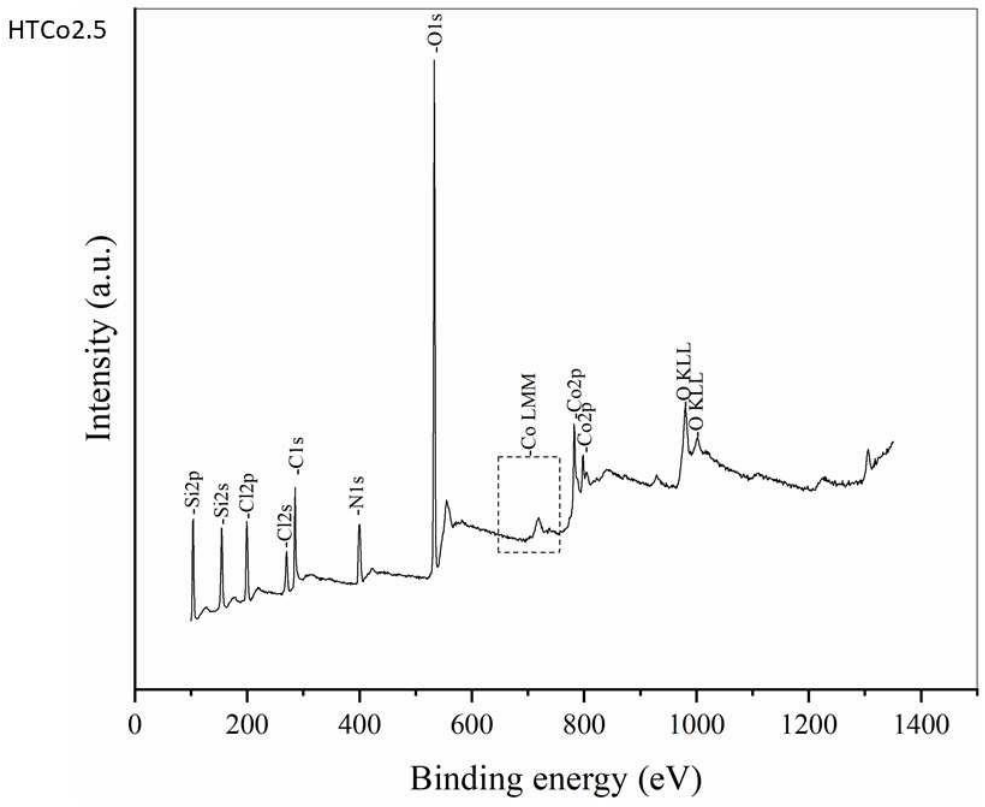

Source: Author (2023).

Figure 29 – Survey spectrum for PHCo2.5.

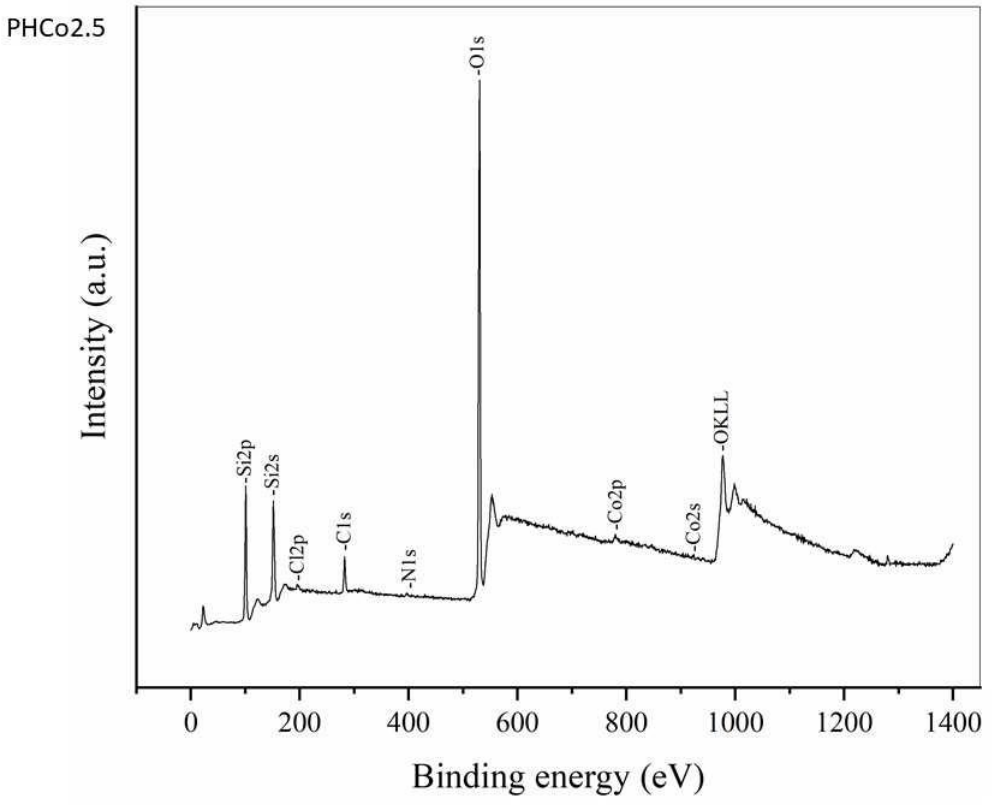

Source: Author (2023).

APPENDIX B – TGA AND DTG RESULTS FOR EACH PRODUCED MATERIAL

Figure 30 – TGA and DTG for AHCo2.5

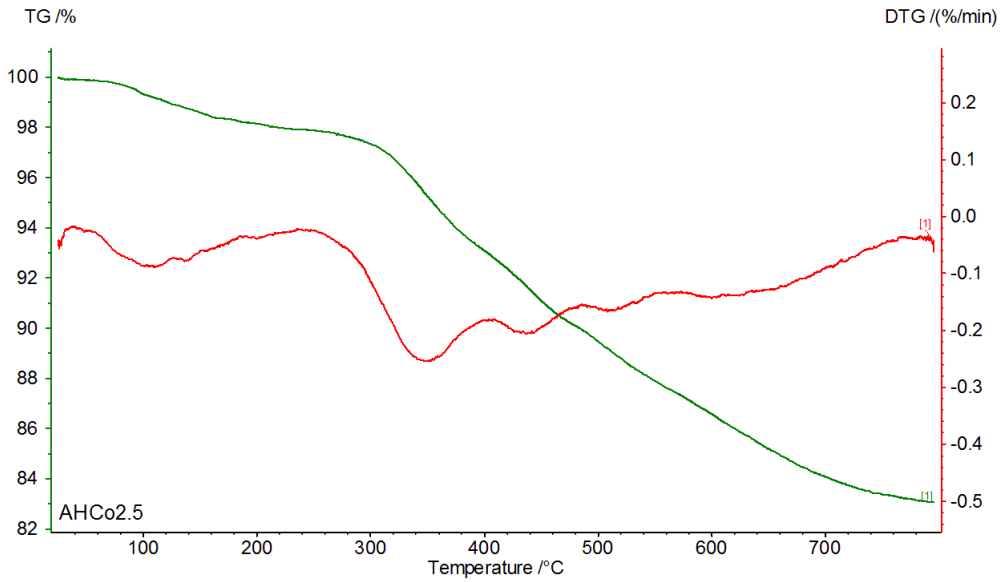

Source: Author (2023).

Figure 31 – TGA and DTG for HTCo2.5

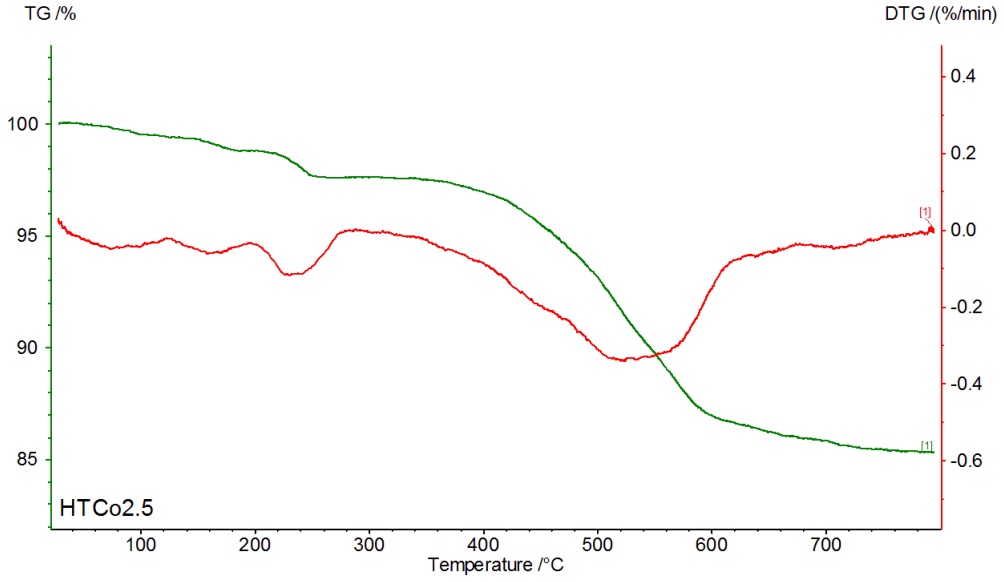

Source: Author (2023).

Figure 32 – TGA and DTG for PHCo2.5

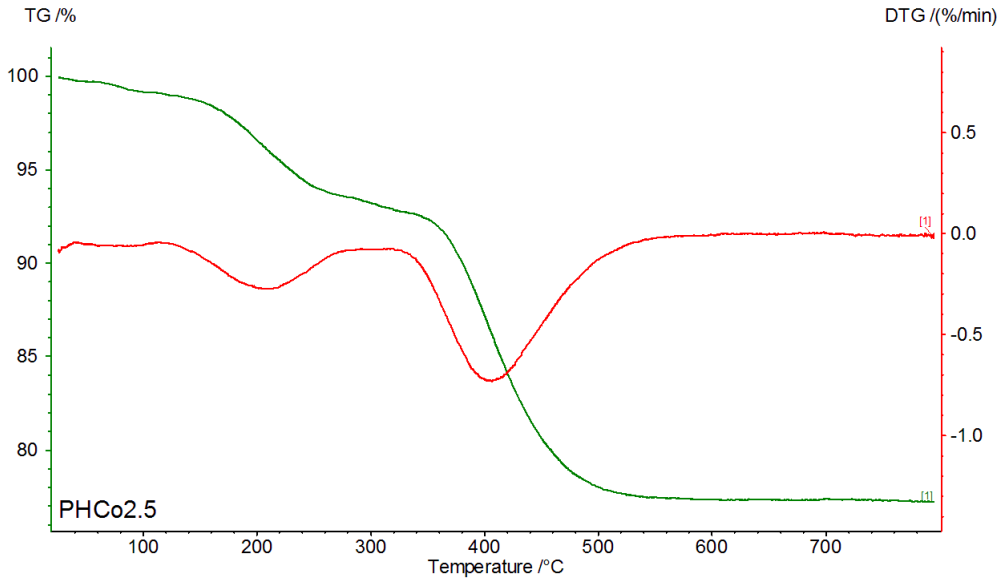

Source: Author (2023).